RL-TR-92-278
Final Technical Report
December 1992

NONLINEAR OPTICS IN THREE LEVEL ATOMIC SYSTEMS

Massachusetts Institute of Technology

Professor S. Ezekiel

APPROVED FOR PUBLIC RELEASE; DISTRIBUTION UNLIMITED.

Rome Laboratory
Air Force Materiel Command
Griffiss Air Force Base, New York

This report has been reviewed by the Rome Laboratory Public Affairs Office (PA) and is releasable to the National Technical Information Service (NTIS). At NTIS it will be releasable to the general public, including foreign nations.

RL-TR-92-278 has been reviewed and is approved for publication.

APPROVED:

Philip R. Hemmer

PHILIP R. HEMMER
Project Engineer

FOR THE COMMANDER:

Harold Roth

HAROLD ROTH, Director
Solid State Sciences
Electromagnetics and Reliability Directorate

If your address has changed or if you wish to be removed from the Rome Laboratory mailing list, or if the addressee is no longer employed by your organization, please notify RL (EROP) Hanscom AFB MA 01731. This will assist us in maintaining a current mailing list.

Do not return copies of this report unless contractual obligations or notices on a specific document require that it be returned.

REPORT DOCUMENTATION PAGE

Form Approved
OMB No. 0704-0188

1. AGENCY USE ONLY (Leave Blank)	2. REPORT DATE	3. REPORT TYPE AND DATES COVERED
	December 1992	Final Jun 89 - May 92

4. TITLE AND SUBTITLE
NONLINEAR OPTICS IN THREE LEVEL ATOMIC SYSTEMS

5. FUNDING NUMBERS
C - F19628-89-K-0030
PE - 62702F
PR - 4600
TA - 19
WU - 77

6. AUTHOR(S)
Prof. S. Ezekiel

7. PERFORMING ORGANIZATION NAME(S) AND ADDRESS(ES)
Massachusetts Institute of Technology
Research Laboratory of Electronics
Cambridge MA 02139

8. PERFORMING ORGANIZATION REPORT NUMBER
N/A

9. SPONSORING/MONITORING AGENCY NAME(S) AND ADDRESS(ES)
Rome Laboratory (EROP)
Hanscom AFB MA 01731-5000

10. SPONSORING/MONITORING AGENCY REPORT NUMBER
RL-TR-92-278

11. SUPPLEMENTARY NOTES
Rome Laboratory Project Engineer: Philip R. Hemmer/EROP/(617) 377-5170

12a. DISTRIBUTION/AVAILABILITY STATEMENT
Approved for public release; distribution unlimited.

12b. DISTRIBUTION CODE

13. ABSTRACT (Maximum 200 words)

The nonlinear optical properties of three-level atomic systems in the resonance Raman configuration are investigated both theoretically and experimentally. Special emphasis is placed on the optical properties which are unique to three-level systems, and have potential device applications. In particular, microwave-phase-dependent optical absorption is demonstrated experimentally. This is of interest because of potential applications to microwave circuit phase mapping, and mm-wave to FIR beam steering and image conversion. Optical data storage with Raman excited microwave spin echoes is also demonstrated experimentally. This technique has potential for increasing storage densities in optical echo memories and may lead to near-room-temperature materials for echo storage and processing. Finally, the optical forces on three-level atoms in Raman resonant standing waves are studied to investigate the potential for using trapped neutral atoms as nonlinear optical elements.

14. SUBJECT TERMS
Nonlinear Optics, Resonance Raman, Atomic Beams

15. NUMBER OF PAGES
64

16. PRICE CODE

17. SECURITY CLASSIFICATION OF REPORT	18. SECURITY CLASSIFICATION OF THIS PAGE	19. SECURITY CLASSIFICATION OF ABSTRACT	20. LIMITATION OF ABSTRACT
UNCLASSIFIED	UNCLASSIFIED	UNCLASSIFIED	UL

ABSTRACT

The nonlinear optical properties of three-level atomic systems in the resonance Raman configuration are investigated both theoretically and experimentally. Special emphasis is placed on the optical properties which are unique to three level systems, and have potential device applications. In particular, microwave-phase-dependent optical absorption is demonstrated experimentally. This is of interest because of potential applications to microwave circuit phase mapping, and mm-wave to FIR beam steering and image conversion. Optical data storage with Raman excited microwave spin echoes is also demonstrated experimentally. This technique has potential for increasing storage densities in optical echo memories and may lead to near-room-temperature materials for echo storage and processing. Finally, the optical forces on three level atoms in Raman resonant standing waves are studied to investigate the potential for using trapped neutral atoms as nonlinear optical elements.

FINAL REPORT

NONLINEAR OPTICS IN THREE LEVEL ATOMIC SYSTEMS

Summary of Objectives

The primary objective of this research program is to investigate the fundamental physical processes underlying nonlinear optical interactions in three level atomic systems. This is accomplished by performing detailed, systematic studies while maintaining close agreement between experimental results and theory. Special emphasis is placed on those optical properties which are unique to three level systems, and which have potential device applications. In particular, three level "Lambda" systems in the resonance Raman configuration are studied because of the existence of optically transparent, long-lived, coherent, quantum superposition states in these systems.

Brief Review of Resonance Raman System and Transparent State

The laser excited resonance Raman interaction is illustrated schematically in Fig. 1. Briefly, the low-lying states $|a\rangle$ and $|b\rangle$ are coupled to a common excited state $|e\rangle$ by two laser fields at frequencies ω_1 and ω_2, respectively. In addition, the two low-lying states can also be coupled directly by a (microwave)

field at frequency ω_3, as shown. In the case of all-optical excitation it is always possible to find a coherent superposition of the low-lying states which is decoupled from the excited state[1] (i.e. transparent to the resonant optical fields). When the low-lying states are metastable, all the atoms become optically pumped into the transparent state[2,3,4]. The result is a decrease in the optical absorption or equivalently in the fluorescence of the excited state, as shown in Fig. 2.

For nonlinear optical applications, the important feature of the transparent Raman coherent state is its sensitivity to the relative phase of the optical laser fields. This is important because it is usually assumed that a two-level system is responsible for nonlinear optical interactions in atoms. However, the optical dipole moments induced in a two level system decay rapidly (typically nanoseconds to milliseconds), so that large photon flux (high laser intensity) is needed to observe nonlinear phenomena. The Raman transparent state, in contrast, can survive much longer than the excited state lifetime ,thereby enabling nonlinear optical interactions to occur at much lower laser intensities.

References -- brief review

[1] H. R. Gray, R. M. Whitley, and C. R. Stroud, Jr., Opt. Lett. 3, 218 (1978).

[2] J. E. Thomas, P. R. Hemmer, S. Ezekiel, C. C. Leiby, Jr., R. H. Picard, and C. R. Willis, Phys. Rev. Lett. 48, 867 (1981).

[3] G. Alzetta, A. Gozzini, L. Moi, and G. Orriols, Nuovo Cimento 36B, 5 (1976).

[4] P. M. Radmore and P. L. Knight, J. Phys. B. 15, 3405 (1982)

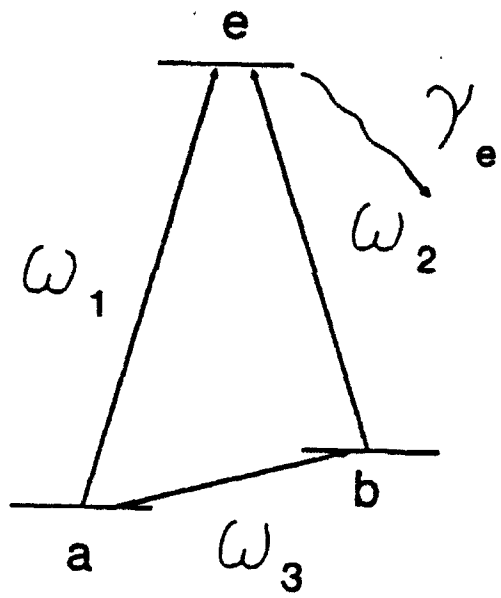

Fig. 1 Schematic of resonance Raman system with direct (microwave) coupling between low-lying states

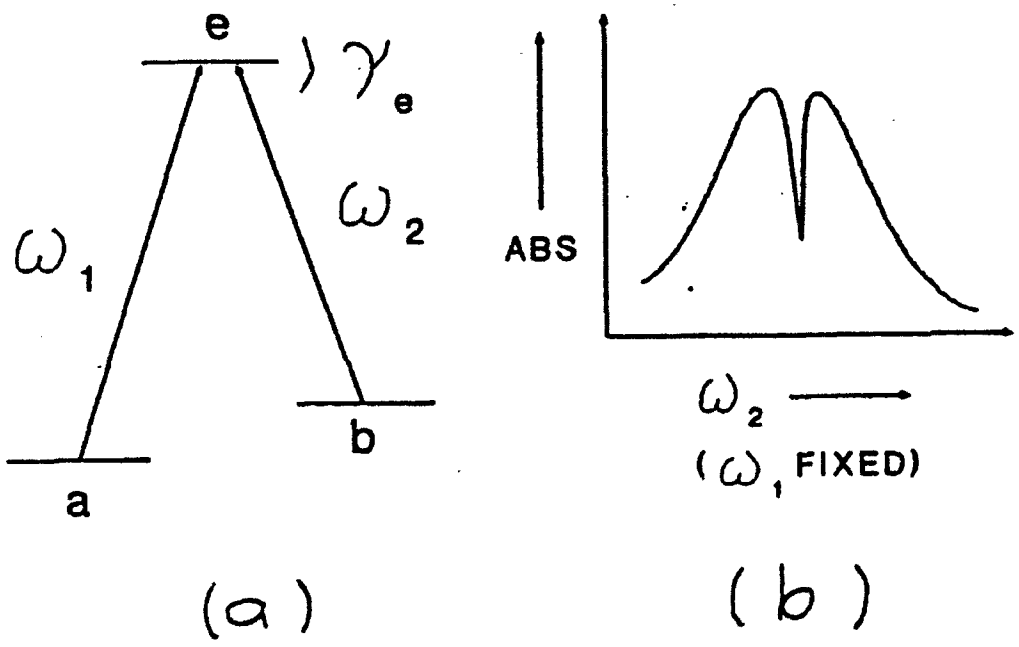

Fig. 2 (a) Resonant Raman system with all-optical excitation. (b) Experimental absorption (fluorescence) lineshape showing induced transparency. Broad feature is resonant absorption lineshape. Narrow feature is absorption dip (transparency).

Results

Research under this program concentrates on three major topics: forces on three level atoms in Raman resonant standing wave optical fields, microwave-phase-dependent optical absorption, and optically excited microwave spin echoes. Each of these topics are discussed separately in the remainder of this report.

(I) Forces on Three Level Atoms in Raman Resonant Standing Wave Optical Fields

The ideal nonlinear optical material is an ensemble of non-interacting atoms, driven near resonance. In existing materials, interactions between atoms and the environment significantly weaken the resonant nonlinear optical response. One way around this problem is to devise a novel nonlinear optical medium which consists of atoms stored in a neutral atom trap. Unfortunately, existing atom traps are sufficiently shallow that the nonlinear optical interaction can easily generate forces which are large enough to eject atoms from the trap, thereby preventing cw operation. Thus, what is needed is a new type of trap, based on the Raman transparent state, which permits cw nonlinear optical interactions. To this end, the optical forces exerted on three level atoms by Raman resonant fields is studied both theoretically and experimentally.

(A) Theory of Optical Forces on the Raman Transparent State in Two Standing Waves

The appropriate atomic level diagram is shown in Fig. I-A-1. In this figure, the detunings of the laser fields at ω_1 and ω_2 are expressed in terms of common mode (correlated) detuning δ and laser difference detuning Δ, defined as follows:

$$\delta = (\delta_1 + \delta_2)/2$$

$$\Delta = \delta_1 - \delta_2$$

As mentioned earlier, it is always possible to find a superposition of low-lying atomic states which are transparent to the resonant optical fields. In the case when the laser difference detuning Δ is zero, all the atoms are optically pumped into the transparent state where they remain indefinitely (for long lived low-lying states). To take advantage of this, we choose to express the Raman interaction in a representation wherein the transparent (or dark) state is one of the basis states. The dark state $|->$ and its orthogonal complement $|+>$ are given as follows:

$$|-> = (g_2|a> - g_1|b>)/g$$

$$|+> = (g_1|a> + g_2|b>)/g$$

where g_1 and g_2 are the Rabi frequencies corresponding to the a <--> e and b <--> e transitions, respectively, and $g = \sqrt{(g_1^2 + g_2^2)}$. For standing wave optical fields, the Rabi frequencies take the following form:

$$g_1 = g_{10}\sin(kx)$$

$$g_2 = g_{20}\sin(kx + \chi)$$

For simplicity, we consider only equal strength standing waves, so that $g_{10} = g_{20} = g_0$. Also, the standing wave phase shift χ is assumed constant on the optical wavelength scale.

In one dimension, the Lorentz force is written as $F = tr(\rho f)$. Here, ρ is the density operator and f is the force operator given by the product of the dipole operator and the gradient of the electric field, $f = -\mu\nabla E$. For the system of Fig. I-A-1, the non-zero elements of f are given, in the rotating wave approximation, by the gradients of the Rabi frequencies:

$$f_{ea} = f_{ae}^{*} = \nabla g_1, \qquad f_{eb} = f_{be}^{*} = \nabla g_2, \qquad (\hbar = 1).$$

To see how this dark state basis simplifies the interaction, consider its Hamiltonian. To obtain this, we first write down the Hamiltonian in the |a>, |b>, and |e> basis:

$$H = (1/2)\begin{bmatrix} \Delta & 0 & -g_1 \\ 0 & -\Delta & -g_2 \\ -g_1 & -g_2 & -2\delta \end{bmatrix}.$$

where the zero of energy is chosen such that $\omega_e + 2\delta = 0$. This Hamiltonian can be obtained by inspection from Fig. I-A-1. Next, we note that the $|->$ and $|+>$ states can be expressed as a rotation of the $|a>$ and $|b>$ states, where the rotation angle θ is defined by $\tan\theta = g_1/g_2$. Making the appropriate transformations gives the Hamiltonian in the $|->$, $|+>$ and $|e>$ basis:

$$H = (1/2)\begin{bmatrix} \Delta\cos(2\theta) & \Delta\sin(2\theta) & 0 \\ \Delta\sin(2\theta) & -\Delta\cos(2\theta) & -g \\ 0 & -g & -2\delta \end{bmatrix}.$$

Now consider the force operator f in the dark state basis. The nonzero elements are:

$$f_{e-} = f^*_{-e} = (g_2\nabla g_1 - g_1\nabla g_2)/g = g\nabla\theta$$

$$f_{e+} = f^*_{+e} = (g_1\nabla g_1 + g_2\nabla g_2)/g = \nabla g$$

where f_{e-} and f_{e+} are real for pure standing wave excitation. These elements can be derived by inspection by noting that the force operator corresponding to the $|->$ state, for example, is

simply a weighted sum of the |a> and |b> state force operators where the weights are the same as in the definition of the |-> state.

Using the results so far gives the following explicit form for the force on a three level atom in standing wave fields:

$$F = f_{e-}Re(\rho_{-e}) + f_{e+}Re(\rho_{+e})$$

We now compute the optical force by estimating the steady-state values of the density matrix elements in several limiting cases. Consider the case when $\Delta\sin(2\theta)$ is non-zero but small compared to the optical pumping rate, g^2/Γ. In this limit, the nonzero density matrix elements can be obtained by perturbing around the $\rho_{--} = 1$ solution. To simplify the analysis further we make the additional approximation that $g \ll \Gamma$, and ignore the influx of atoms into the |+> and |-> states from the |e> state. This allows us to avoid solving the complex density matrix equations (OBE's) entirely, by instead representing the system with a wave function of the form $\Psi = A_-|->+A_+|+>+A_e|e>$.

The dynamics of the system is now contained in the |->, |+>, |e> state amplitudes, whose equations of motion are given by the Schrodinger equation:

$$\frac{\partial}{\partial t}\begin{bmatrix} A_- \\ A_+ \\ A_e \end{bmatrix} = (-i/2)\begin{bmatrix} \Delta_c & \Delta_s & 0 \\ \Delta_s & -\Delta_c & -g \\ 0 & -g & -i(\Gamma - 2i\delta) \end{bmatrix}\begin{bmatrix} A_- \\ A_+ \\ A_e \end{bmatrix}$$

where $\Delta_c = \Delta\cos(2\theta)$, $\Delta_s = \Delta\sin(2\theta)$, and the phenomenological damping Γ is added to the Hamiltonian. The Raman interaction in this new basis is illustrated in Fig. I-A-2(a)

Since $\Gamma \gg g$, we can use the adiabatic following approximation[1,2,3], to solve for A_e. The result is $A_e = -i(g/\Gamma_\delta)A_+$, where $\Gamma_\delta = \Gamma - 2i\delta$. Using this result to eliminate A_e, the wave function now becomes, $\Psi = A_-|->+A_+|+>_d$. The new basis state $|+>_d = |+> - i(g/\Gamma_\delta)|e>$ is called the damped state. In the adiabatic limit, the dark and damped states form a closed two level system, as illustrated in Fig. I-A-2(b).

It is easy to show that the amplitude equations for the dark and damped states are simply:

$$\frac{\partial}{\partial t}\begin{bmatrix} A_- \\ A_+ \end{bmatrix} = (-i/2)\begin{bmatrix} \Delta_c & \Delta_s \\ \Delta_s & -i(\Gamma_+ - i\Delta_c) \end{bmatrix}\begin{bmatrix} A_- \\ A_+ \end{bmatrix}$$

where $\Gamma_+ = g^2/\Gamma_\delta$. Thus, the decay rate of the $|+>_d$ state is the optical pumping rate g^2/Γ_δ, which is proportional to total laser intensity.

To solve the remaining amplitude equations in the limit of $\Delta \ll \Gamma_*$ we can again make the adiabatic approximation to solve for A_{*}. The result is $A_* = i[\Delta_s/(\Gamma_* - i\Delta_c)]A_-$.

From these results, we can generate the approximate density matrix elements:

$$\rho_{-e} = \left(\frac{g}{\Gamma_e}\right)\left(\frac{\Delta_s}{\Gamma_* - i\Delta_c}\right), \qquad \rho_{*e} = -i\left(\frac{g}{\Gamma_e}\right)\rho_{**}, \qquad \rho_{**} = \left|\frac{\Delta_s}{\Gamma_* - i\Delta_c}\right|^2$$

where again $\rho_{--} \cong 1$ has been assumed. Substituting these into the force expression and remembering the approximations $\Delta \ll \Gamma_* \ll \Gamma$ gives:

$$F = f_e \cdot Re(\rho_{-e}) = 2\Delta g_1 g_2 (g_2 \nabla g_1 - g_1 \nabla g_2)/g^4$$

where the additional approximation of $\delta \ll \Gamma$ has been used. It should be noted that the |+> state contribution to the force is negligible for these approximations. Thus, the force on a three level atom, in this limit, is due entirely to the force on the |-> or dark state. Also note that the force is independent of δ (for $\delta \ll \Gamma$). This is related to the fact that the Raman induced transparency is independent of δ.

This force expression is plotted and compared to the OBE solution in Fig. I-A-3, for the case of two standing waves (SW)

with equal amplitudes ($=g_0$), i.e., $g_1 = g_0 \sin(kz)$ and $g_2 = g_0 \sin(kz+\chi)$, where $k = k_1 = k_2$. The phase difference is chosen to be $\chi = \pi/4$. Specifically, Fig. I-A-3(a) shows a plot of the two SW field amplitudes. The solid curve in Fig. I-A-3(b) is a plot of the above force expression and the circles correspond to the optical Bloch equation (OBE) solution. As can be seen, the lowest order force estimate agrees well with the OBE result.

Note that the force in the Λ system shows sub-optical-wavelength behavior. In addition, the force can also show strong rectification (i.e., non-zero value when averaged over an optical wavelength). One case where the origin of this rectification can be clearly illustrated is when the difference detuning is large enough to saturate the $|->\rightarrow|+>_d$ transition.

For simplicity, we set $\delta = 0$ in this discussion, so that $\Gamma_\delta = \Gamma$ and $\Gamma_s = g^2/\Gamma$ is purely real. When the $|->\rightarrow|+>_d$ transition is saturated, the second adiabatic following approximation is no longer valid. However, the $|->$ and $|+>_d$ system is effectively a closed two-level system, so that its steady state density matrix elements can be written by inspection of the amplitude equations:

$$\rho_{-+} = -i\left(\frac{\Delta_s}{\Gamma_s - 2i\Delta_c}\right)\ (\rho_{--} - \rho_{++}),$$

$$(\rho_{--}-\rho_{++})=\frac{\Gamma_*^2+4\Delta_c^2}{\Gamma_*^2+4\Delta_s^2+4\Delta_c^2}.$$

Remembering the first adiabatic approximation then gives:

$$Re(\rho_{-e})=Re\left[\left(\frac{A_e}{A_*}\right)^*\rho_{-+}\right]=\left(\frac{g}{\Gamma}\right)\frac{\Delta_s\Gamma_*}{\Gamma_*^2+4\Delta^2},$$

where use has been made of the identity $\Delta_s^2+\Delta_c^2=\Delta^2$.

In the limit of $|\Delta|\ll\Gamma_*$ this result reduces to that obtained using the second adiabatic following approximation, as expected. However, in the opposite limit of $|\Delta|\gg|\Gamma_*|$ (but $|\Delta|\ll g$), the force becomes

$$F=\frac{[g_1g_2][g_2\nabla g_1-g_1\nabla g_2]}{2\Delta\Gamma^2}=\frac{kg_0^4[\mathrm{Cos}\chi-\mathrm{Cos}(2kz+\chi)][\mathrm{Sin}\chi]}{4\Delta\Gamma^2}$$

Here, the $(g_2\nabla g_1-g_1\nabla g_2)$ term arises from the force operator. This term reduces to $g_0^2\mathrm{Sin}\chi$, which is effectively constant over an optical wavelength. In contrast, the $g_1g_2=(g_0^2/2)[\mathrm{Cos}\chi-\mathrm{Cos}(2kz+\chi)]$ term, which comes from the ρ_{-e} coherence, is not a constant over an optical wavelength. However, it has a component $(\mathrm{Cos}\chi)$ which is a constant. The other component of ρ_{-e}, $[\mathrm{Cos}(2kz+\chi)]$ is periodic over an optical wavelength. Therefore, when averaged over an optical wavelength,

the force is proportional to $\mathrm{Sin}(2\chi)$. This rectified force as a function of χ is shown by the solid line in Fig. I-A-4. The dotted curve in the figure is the rectified force computed using the exact solution of the OBE's. Again, reasonably good agreement is seen.

For other values of laser difference detuning and Rabi frequency, the OBE's must be solved exactly to find the force. An example of this is shown in Fig. I-A-5 for the $\delta = 0$ case. As can be seen, the optical force is totally rectified for this particular choice of parameters. The rectified component of this force (dashed line in the figure) is periodic over half the beat wavelength, as shown in Fig. I-A-6. It is important to note that the force also displays features which are much narrower than an optical wavelength (see Fig. I-A-5). Further calculations are needed to determine the implications of these narrow structures to nonlinear optical interactions.

To summarize, we have used the normal modes of the atom-field to physically model the origins of novel structures that appear in the force on a Λ system atom under standing wave excitation. In particular, we have identified a situation where the force is only on the dark state, thus leading to simple, closed form expressions for the force. Finally, our estimated results agree well with solutions of the OBE's in the regions

where the approximations used are valid.

References -- part I-A

[1] P.R.Hemmer, G.P.Ontai and S.Ezekiel, **JOSAB** 3, 219 (1986)

[2] P.R. Hemmer, M. G. Prentiss, **JOSAB** 5, 1613 (1988)

[3] P.R.Hemmer, M.S.Shahriar, V.D.Natoli and S.Ezekiel, **JOSAB** 6, 1519 (1989)

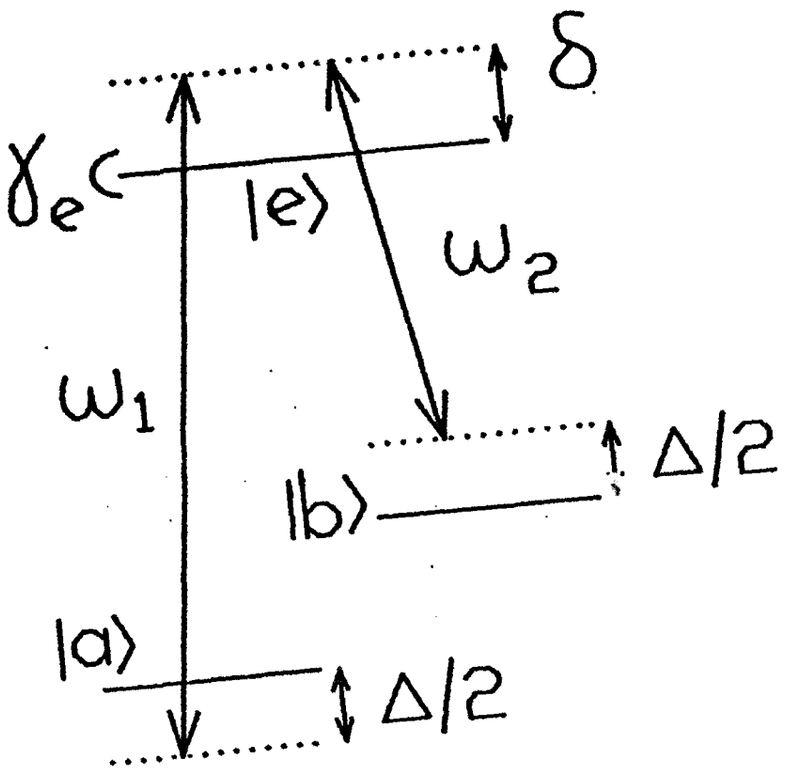

Fig. I-A-1 Schematic of resonance Raman system including laser detunings.

Fig. I-A-2 (a) Resonance Raman system in dark state basis, for $g_1 = g_2$ (b) Equivalent two-level system which describes the resonance Raman interaction in the limit of weak Rabi frequencies.

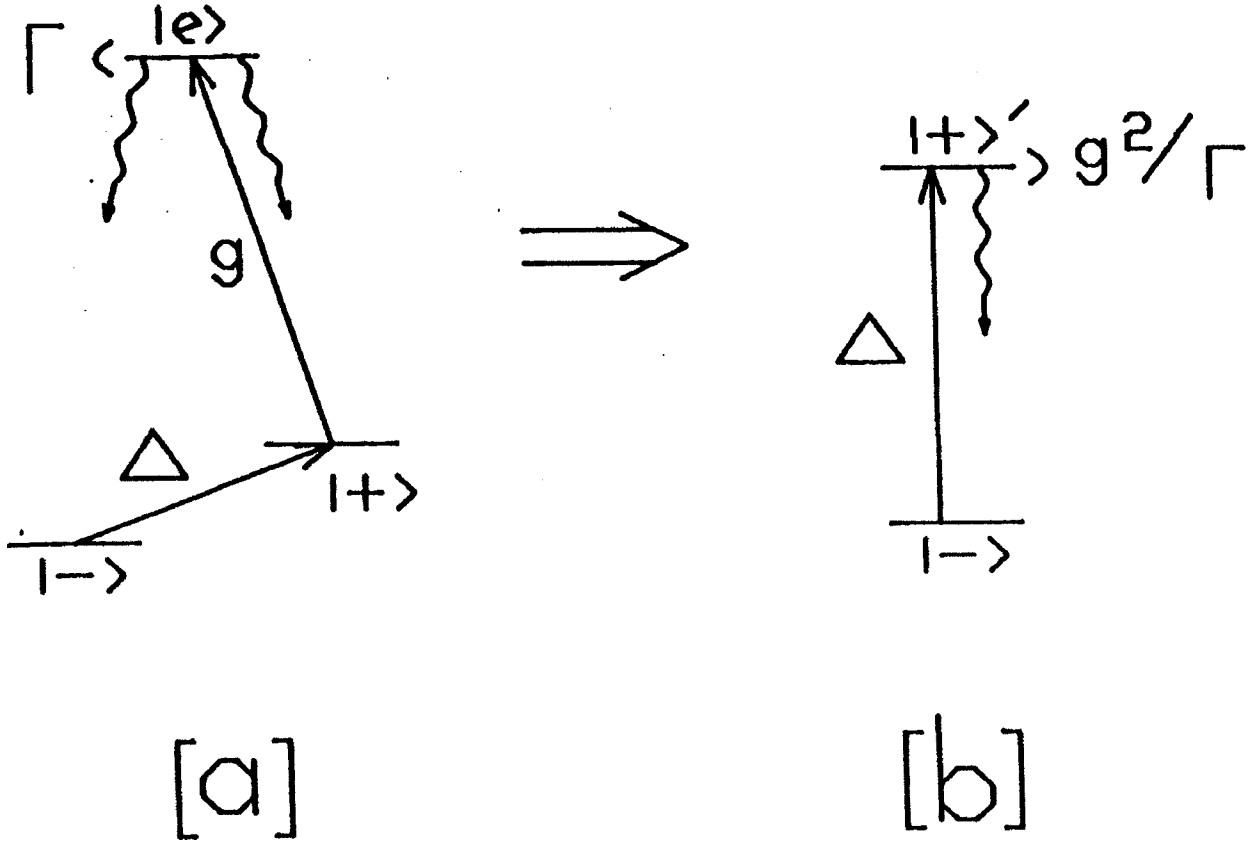

Fig. I-A-3 (a) Rabi frequencies for standing wave optical fields having a phase difference of $\chi = \pi/4$. (b) Optical force in the limit of $|\Delta| \ll |\Gamma_1|$. Solid curve is experession derived in text. Circles are from exact optical Bloch equation solution.

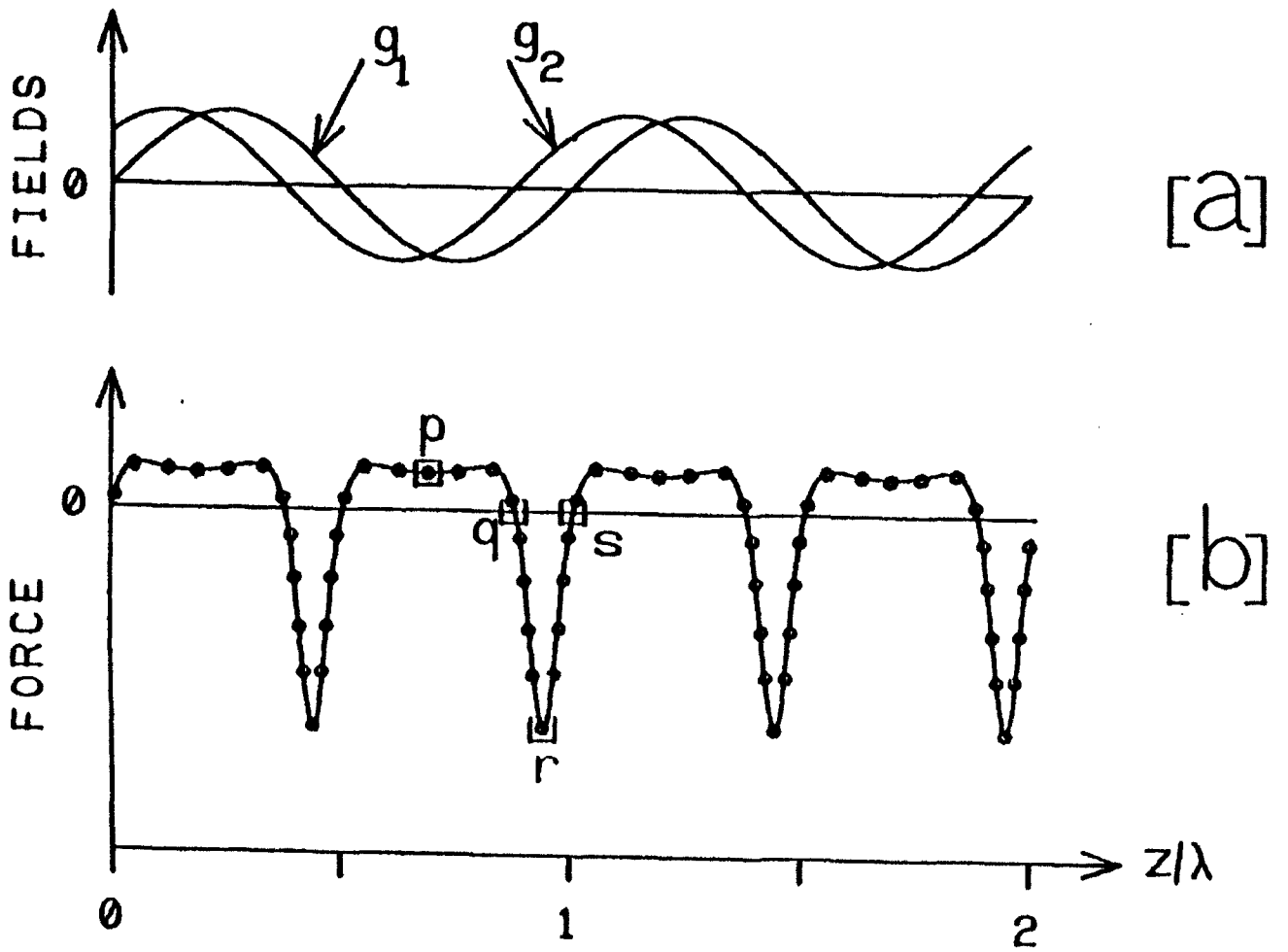

Fig. I-A-4 Rectified optical force vs. standing wave phase χ. Solid curve is estimate when $g \gg |\Delta| \gg |\Gamma_e|$. Dotted curve is optical Bloch solution. For each plot, $g_0 = 3.3\Delta = 0.1\Gamma_e$.

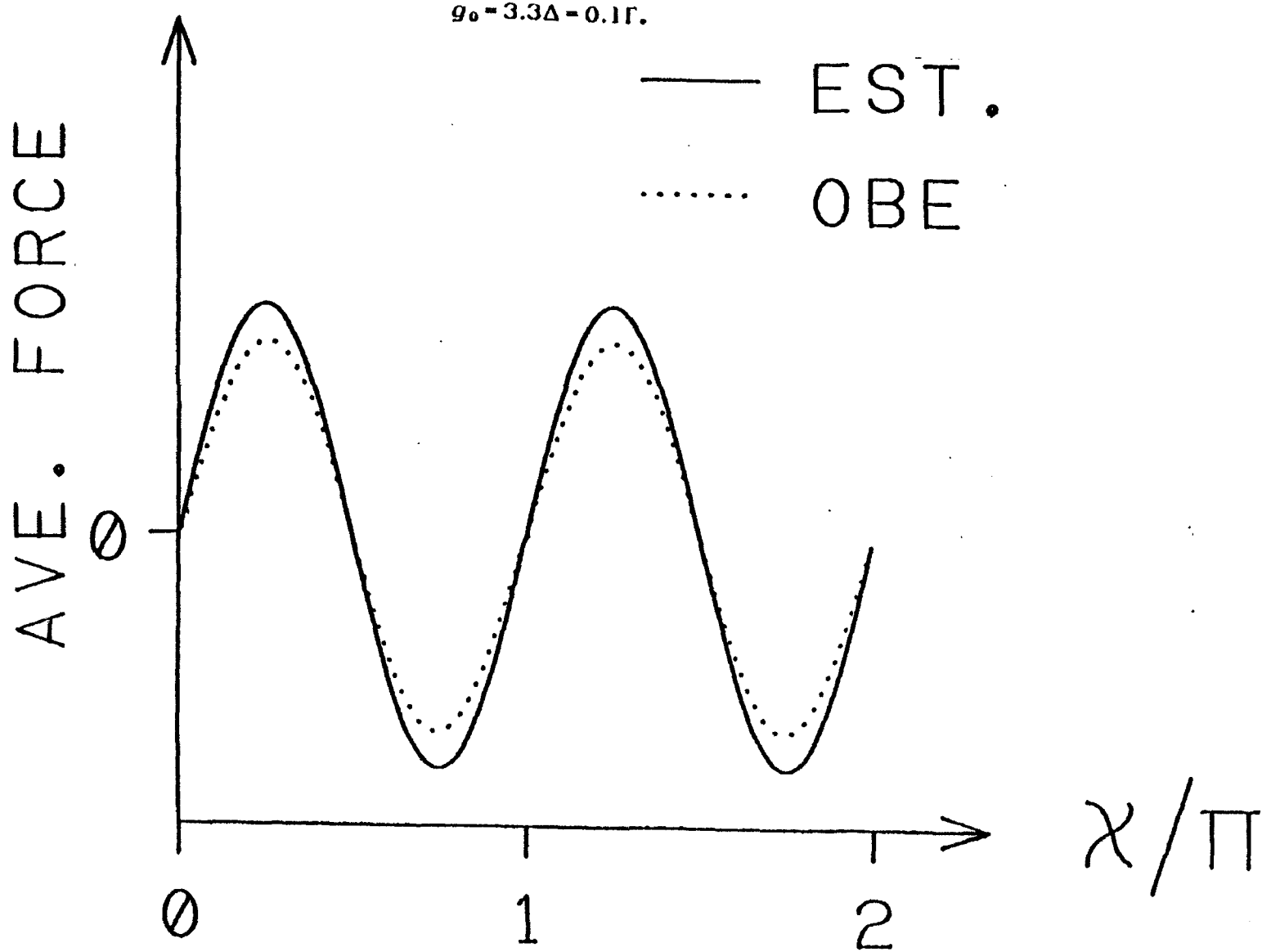

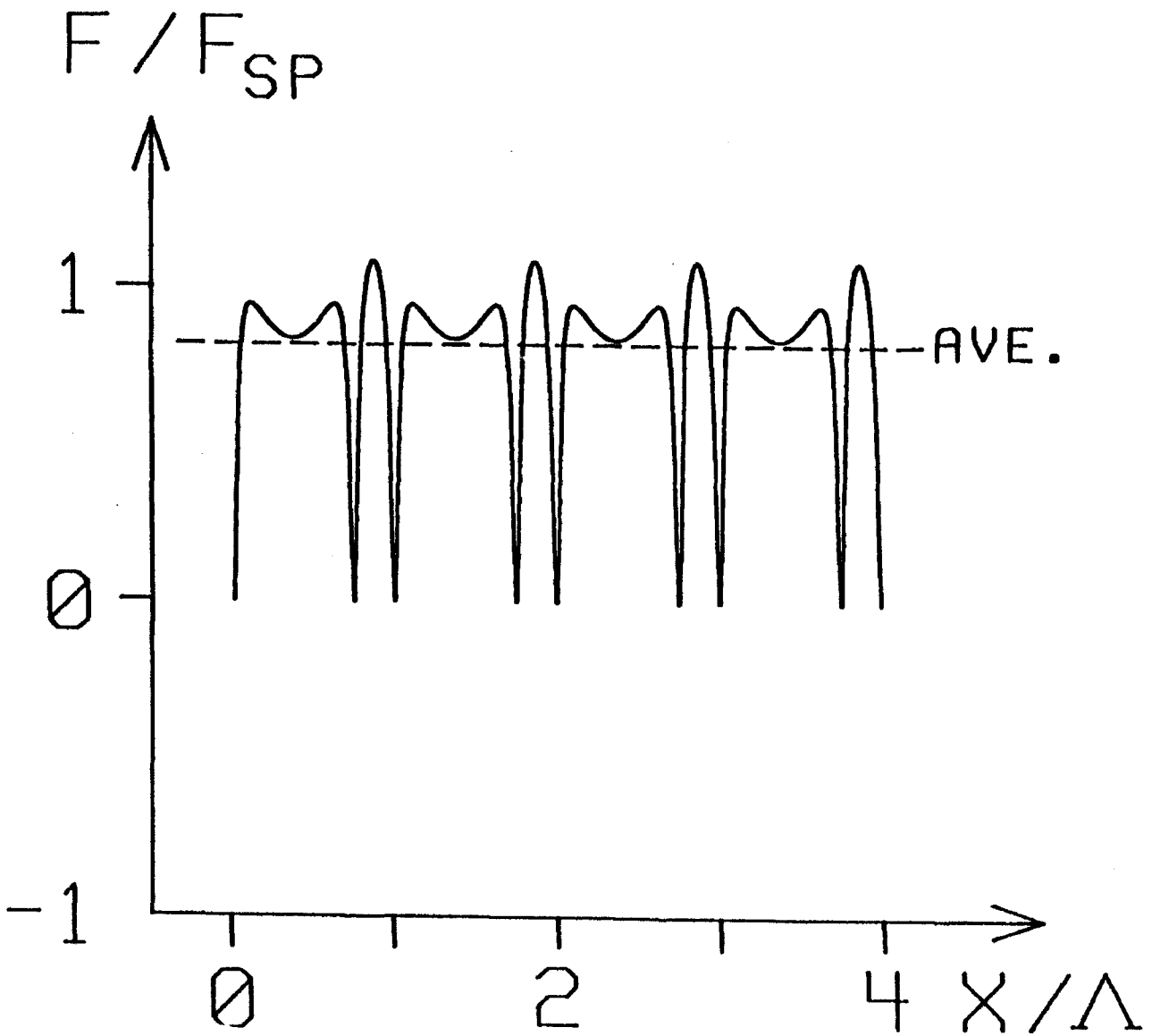

Fig. I-A-5 Force on optical wavelength scale for $\delta = 0, \Delta = g_0/2 = 4\Gamma$ and $\chi = \pi/4, F_{sp} = \hbar\Gamma/\lambda_{opt}$. Dashed line is spatially avaraged force.

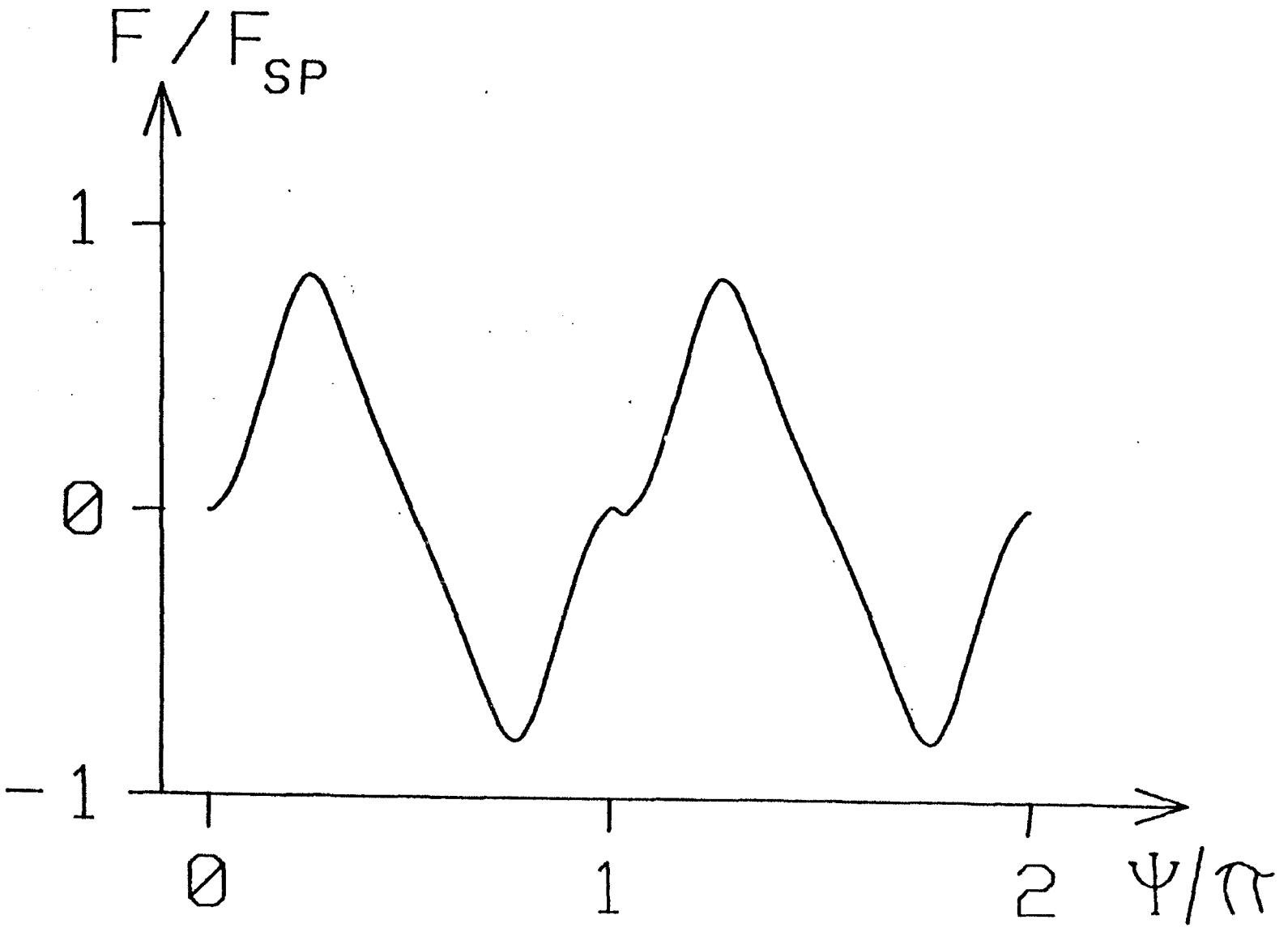

Fig. I-A-6 Spatially avaraged force vs. standing wave phase shift $\Psi(=\chi)$ for parameters of Fig. I-A-5.

(B) First Observation of Deflection and Cooling of Three-level Atoms in Raman Resonant Standing Wave Optical Fields

Here we show experimental verification of the existence of the long range component of the force on three-level atoms by deflecting an atomic beam of sodium atoms using two Raman resonant standing wave laser fields. The long range force is defined as the force averaged over an optical wavelength. In addition, we show the existence of damping forces. These observations are important for several reasons. First, the deflecting force is stimulated, so that it can be made arbitrarily large. With the co-existence of semiclassical damping forces, this opens the possibility of developing a neutral atom trap in which both the damping and the restoring forces are optical. Since the restoring force is stimulated in nature, such trap would be possibly much deeper than the magneto-optic trap, wherein the restoring force is spontaneous. Second, the Raman interaction tends to drive atoms into the transparent (or "dark") state[1,2]. Atoms in a Raman trap would therefore be mostly in the ground states, so that the collisional lifetime of the atoms would be much longer than in magneto-optic traps. As a result, the Raman force may ultimately lead to high densities of cold and dark

atoms in traps. Such a dense collection of atoms in transparent superposition states could find applications as novel, low intensity nonlinear optical materials[3,4].

The schematic diagram of the three level Λ system is shown in Fig. I-B-1(a). In this experiment, the states $|a\rangle$ and $|b\rangle$ are, respectively, the F = 1 and F = 2 hyperfine components (1772 MHz separation) of the $3^2S_{1/2}$ sodium ground state and are coupled to the excited state $|e\rangle$ by laser fields at ω_1 and ω_2 (near 590 nm), as shown. State $|e\rangle$ is the F = 2 component of the $^3P_{1/2}$ excited state (D1 line) which decays at a rate Γ = 10 MHz. As before, laser detunings are expressed in terms of common mode (or correlated) detuning δ and difference frequency detuning Δ, defined respectively as $\delta=(\delta_1+\delta_2)/2$ and $\Delta=(\delta_1-\delta_2)$, where δ_i is the detuning of the field at ω_i.

The optical Bloch equations can be solved to give the force exerted by two standing wave fields on the three level system shown in Fig. I-B-1(a). For co-linear optical standing waves, the Rabi frequencies can be written as $g_1 = g_1^0\sin(kz)$ and $g_2 = g_2^0\sin(kz + \chi)$ where $k=k_1=\omega_1/c$ and $\chi=(k_2-k_1)z$ is the phase difference between the optical standing waves and z is the position of the atom. It can be shown that for conditions corresponding to our experiment (e.g. g_1^0, g_2^0 and Δ comparable to Γ) the long range component of this force varies basically as $\sin(2\chi)$, and

its sign is proportional to the sign of Δ. Thus, the force is anti-symmetric with respect to Δ, zero when $\chi = n\pi/2$ (n is any integer), and anti-symmetric with respect to χ about these zeros.

The experimental setup used to observe atomic beam deflection is shown schematically in Fig. I-B-1(b). A sodium oven at 400°C is used to generate the atomic beam which is collimated to about 3 mrad (FWHM) by two 1.5 mm diameter pinholes separated by 55 cm. Windows are provided in the atomic beam apparatus for a deflection zone (labeled D in Fig. I-B-1(b)) and an observation zone (labeled O) 18 cm and 58 cm, respectively, from the second pinhole. An argon pumped ring dye laser is used to generate the optical field at ω_1 (590 nm). The field at ω_2 is generated with an electro-optic phase modulator (E/O_1). To change ω_1 the laser is offset-locked by sending a portion of the laser output through an acousto-optic modulator (A/O) followed by a second E/O (E/O_2), as shown, to generate nearly equal (about 980 MHz) but opposite frequency shifts. The output of the A/O and E/O_2 combination is then locked to an atomic beam reference (labeled REF) so that by changing the frequency of the A/O, both ω_1 and ω_2 are tuned together (correlated detuning). The laser emerging from E/O_1 is expanded to a line with a length of 4.1 cm and a width of about 0.24 mm (FWHM) at the atomic beam. A translatable mirror on the

opposite side of the atomic beam retroreflects the deflecting laser beam. Maximum laser power (all frequencies) in the incoming deflecting beam is about 70 mW.

To detect the atomic beam deflection, a portion of the reference laser beam (from the A/O and E/O combination) is split off to form a standing wave probe field which intersects the atomic beam in the observation region. To avoid Doppler shifts the probe beam is made perpendicular to both the deflecting laser beam and the atomic beam. Fluorescence generated by this probe field is imaged onto a CCD video camera, as shown.

Atomic beam deflection data obtained with the setup of Fig. I-B-1(b) are shown in Fig. I-B-2. Each data trace is a digitized line trace from a single stored video frame. Since the deflecting laser beam width is smaller than that of the atomic beam, only the central portion of the atomic beam is deflected. The line traces shown in Fig. I-B-2 correspond to the vertical positions in the video frames which give maximum deflection. For this data we chose to use the maximum laser power available (200mW/cm2) in the deflection zone. The detunings were then optimized (Δ = -16 MHz, δ = 4.4 MHz) to observe the cleanest deflection.

In Fig. I-B-2 the top trace shows the atomic beam profile with the deflecting laser blocked. The next four traces show the

deflection obtained for standing wave fields having relative phase shifts of $\chi = 0$, $\pi/4$, $\pi/2$, and $3\pi/4$ as labeled. The $\chi = 0$ trace, which corresponds to in phase standing waves, is obtained with the retroreflecting mirror 17 cm (or one complete optical beat wavelength) from the atomic beam. Moving the mirror progressively closer to the atomic beam results in the increasing values of χ used to obtain Fig. I-B-2. Finally, the bottom trace in the figure is obtained with the retroreflected deflecting laser beam blocked. This data trace shows the spontaneous deflection induced by copropagating travelling waves at ω_1 and ω_2, and is included for comparison. The peak atomic beam deflection in this case is about 5 mrad. Here, it should be noted that the spontaneous force on the three level Λ system is always smaller than the spontaneous force on a two level system because of the effects of coherent population trapping.

Examination of the data in Fig. I-B-2 reveals several important points. First, the atomic beam profile for $\chi = \pi/4$ shows clear asymmetry and centroid deflection to the left, which is the direction of the incoming deflecting laser beam. In contrast, for $\chi = 3\pi/4$, the asymmetry and centroid shift are similar in magnitude, but in the opposite direction. For $\chi = 0$ and $\pi/2$, the centroids are not shifted. Reversal of asymmetry and centroid shift are also observed (not shown) for fixed values of χ (e.g. $\chi = \pi/4$ or $3\pi/4$) when the laser difference detuning Δ is reversed

in sign. However, for the Raman travelling waves the deflection is not reversed. These observations are in agreement with theoretical predictions.

Quantitative comparison of the magnitudes of the observed deflections in Fig. I-B-2 with theory is difficult for two reasons: First, sodium is not a pure three level system but rather has 13 m-levels with 21 allowed optical transitions for the laser polarization and magnetic field orientation used in this experiment. Since each optical transition has a different matrix element, different Rabi frequencies apply. Second, the observed peak deflection angle (when $\chi = \pi/4$ or $3\pi/4$) is about 4 mrad, which corresponds to a final transverse velocity of about 280 cm/s or a Doppler shift of about $\Gamma/2 = 5$ MHz. Since this is comparable to Δ, g, and Γ, the $v = 0$ assumption used to derive the theoretical force is not strictly valid. Nonetheless, to get an idea about the size of the deflection, we have used the v=0 approximation to find the force for a representative transition ($^2S_{1/2}$,F=1,m_F=0 --> $^2P_{1/2}$,F=2,m_F=1 --> $^2S_{1/2}$,F=2,m_F=0). Assuming this force to remain constant over the deflection zone, we find a maximum deflection (at $\chi = \pi/4$ or $3\pi/4$) of 5.6 mrad, which is consistent with the observed maximum deflection of about 4 mrad.

As we have pointed out, the deflection force changes sign when the sign of Δ is reversed. This property can be of help in

designing an all optical trap. Briefly, one can conceivably design a B-field gradient such that the value of Δ is anti- symmetric with respect to the zero field point , which would be the trap center. The dimension of the trap is to be small enough (compared to 17cm) so that the value of χ remains a constant (e.g., $3\pi/4$). The deflection force would thus always push the atoms towards the trap center, thus acting as a restoring force. Generalizing this scheme to three dimensions is of course a non-trivial problem. However, three dimensional generalizations have been found for the case of travelling wave Raman excitations, which can possibly be extended to the standing wave scheme.

Of course, in order for such a trap to work, one would need a mechanism of cooling. To this end, Fig. I-B-3 shows a set of traces obtained under conditions optimized for cooling. The laser intensity here is the same as that in Fig. I-B-2, while the detunings are different (Δ=-3MHz, δ=10.6 MHz). As before, the top trace corresponds to the atomic beam profile with the deflecting beam blocked. The other traces display cooling for two representative phases, $\chi=\pi/2$ and $\chi=3\pi/4$. Note that the cooling is more prominent at $\chi=3\pi/4$. To interpret how strong this cooling is, note that according to the collimation geometry mentioned before, a beam cooled to nearly zero transverse temperature would have a width (FWHM) of about 2.0 mm, which is roughly the width of the beam at $\chi=3\pi/4$. This implies strong cooling at

this phase. An accurate measurement of the amount of cooling therefore would require a beam which is significantly more collimated. We should also point out that such a strong cooling, and the lack of resolution, would tend to mask the observation of the deflecting force that exists at this value according to our theory of v=0 force.

Comparing Fig. I-B-2 with Fig. I-B-3, we find that the optimum deflection and optimum cooling happen for different set of detunings. However, the maximum deflection and the maximum cooling happen at the same phase. Moreover, the cooling is optimum for a smaller value of Δ, which would be nearer to the center of the aforementioned trap. On the other hand, the deflection force is optimum for bigger values of Δ, which would be away from the center. Thus, even though we do not have any direct evidence of cooling and deflection present at the same time, the trap proposed above should in principle work.

In summary, we have observed the phase dependent deflection of a sodium atomic beam by two standing waves, simultaneously near resonance with both components of a Λ three level system. Qualitative agreement between theory and experiment is achieved, even though sodium is not a pure three level system and the stationary atom assumption is violated. In addition, we have observed phase dependent cooling, being maximum at the phase

where the deflection is maximum. Potential applications to high density, dark atom traps are currently being investigated. Such dark atom traps may be useful in nonlinear optics.

References -- part I-B

[1] M. G. Prentiss, N. Bigelow, M. S. Shahriar, P. R. Hemmer, K. Berggren, J. Mervis, S. Ezekiel, Enrico Fermi International School of Physics Course CXVIII, "Laser manipulation of Atoms and Ions," Milan, Italy (July 1991).

[2] P. R. Hemmer, M. G. Prentiss, M. S. Shahriar, N. P. Bigelow, Opt. Comm., accepted.

[3] M. S. Shahriar, P. R. Hemmer, Phys. Rev. Lett., 65, 1865 (1990).

[4] J. Donoghue, M. Cronin-Golomb, J. S. Kane, P. R. Hemmer, Opt. Lett., 16, 1313 (1991).

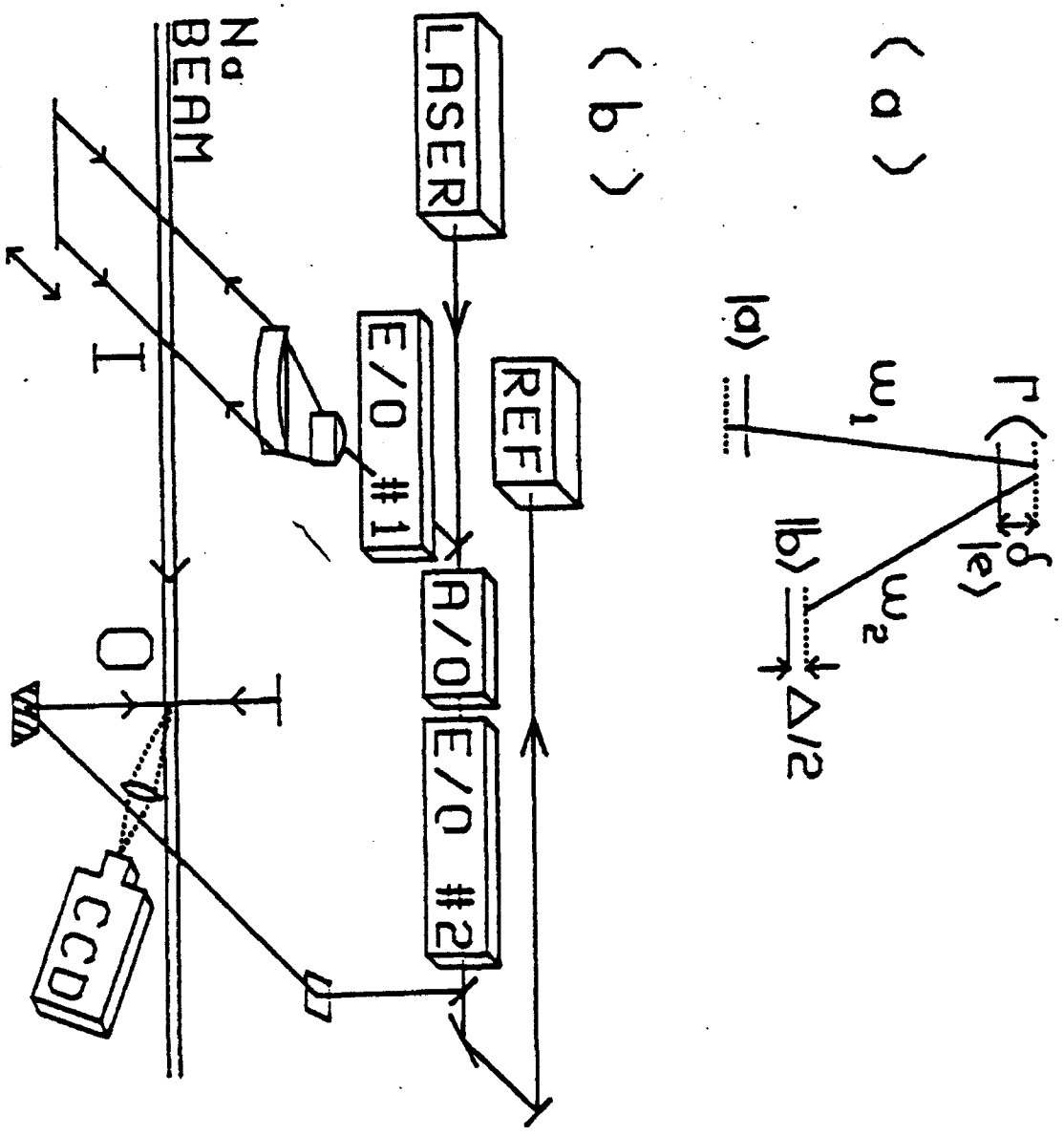

Fig. I-B-1 (a) Schematic of the three level Λ system. (b) Perspective diagram of the experimental setup used to observe atomic beam deflection (deflecting laser beam is perpendicular to atomic beam). D is the deflection zone, O is the observation zone, REF is a reference atomic beam and associated optics, CCD is a charge coupled device video camera.

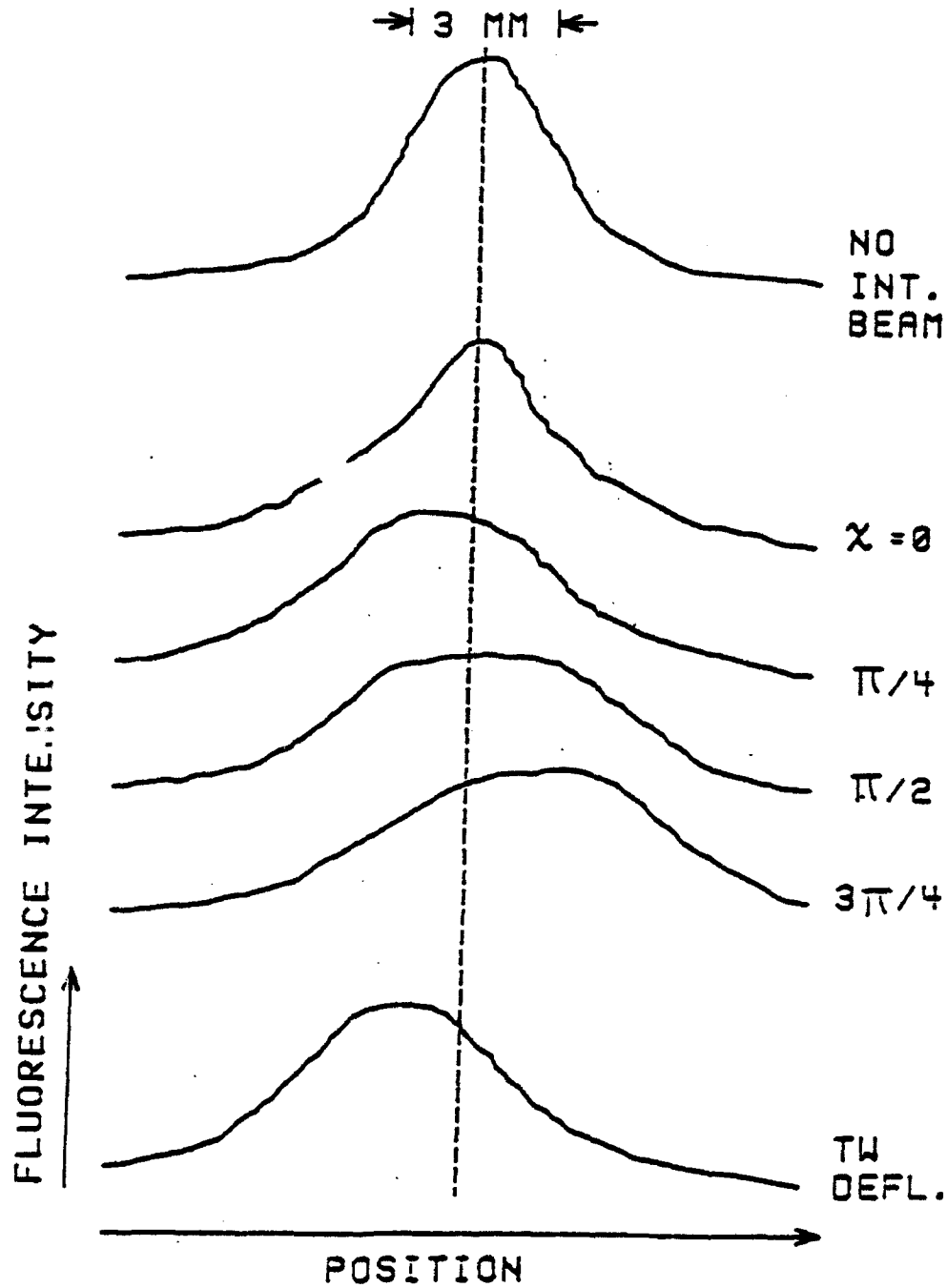

Fig. I-B-2 Data showing atomic beam deflection. Traces are obtained by digitizing single lines of stored video images. From top to bottom: (1) atomic beam in absence of the deflecting beam (2) deflected atomic beam when $\chi = 0$, (3) $\chi = \pi/4$, (4) $\chi = \pi/2$, (5) $\chi = 3\pi/4$, (6) deflected atomic beam for travelling wave optical fields (retroreflected deflecting beam

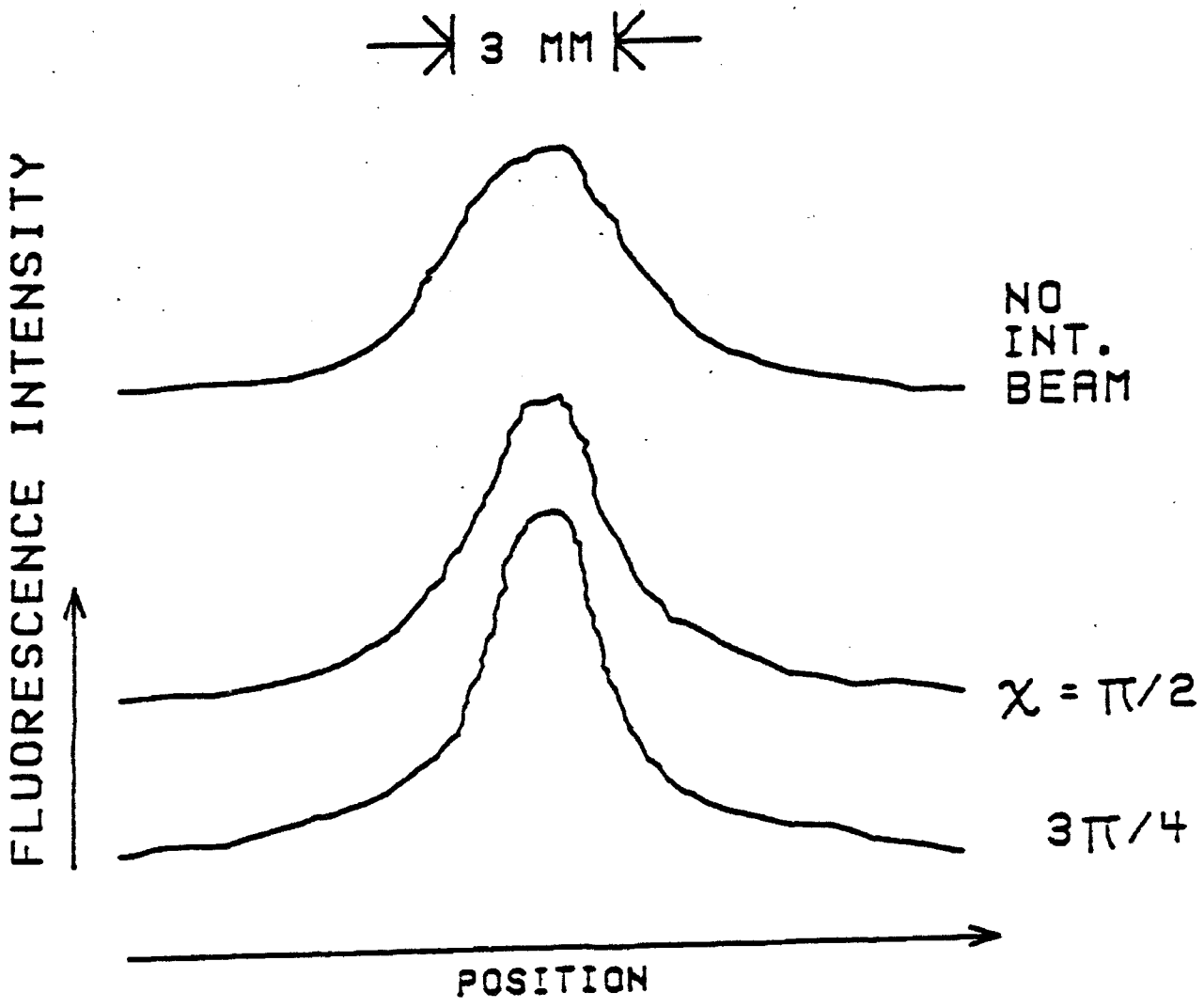

Fig. I-B-3 (a) Data showing cooling, but almost no deflection, which is probably suppressed by the strong cooling, and the limited resolution (b) Data showing heating ($\chi=\pi/2$) and heating with deflection ($\chi=3\pi/4$).

(II) Microwave-Phase-Dependent Optical Absorption

It is well known[1] that in a laser excited resonant Raman interaction atoms are optically pumped into a pure dressed state, the so-called trapped state, which is transparent to the optical excitation fields. In atomic sodium, this trapped state consists of a linear combination of hyperfine sublevels, having a microwave frequency separation. We have demonstrated that in the presence of a resonant microwave field, the Raman trapped state translates into one or the other microwave spin-locked (dressed) state, under appropriate experimental conditions. Analogously, we have shown that a microwave field can also be used to excite the optical Raman trapped state.

Dressed states have been observed before in the microwave[2] and visible wavelength[3] regimes using excitation field phase shifting methods. In addition, the optical Raman trapped state was first observed indirectly, as a fluorescence reduction[4]. However, this is the first time a double optical (Raman) interaction has been employed to excite the dressed state of a single photon (microwave) interaction, and vice versa. This effect is of fundamental interest because it allows optical absorption to be modified by a change of only the phase of a microwave field. Such a phase dependent optical/microwave absorption has numerous potential applications, as will be described later.

Fig. II-1(a) shows a three level atomic system in the Λ configuration where ω_1 and ω_2 are the frequencies of the optical fields and ω_3 is the frequency of the microwave field. Here, it is assumed that states a and b are long-lived, but state e is short lived with a decay rate of γ_e. For long interaction times (no microwave field) the atoms are optically pumped into a non-absorbing trapped dressed state of the form[1,5]:

$$\left(\frac{g_2}{\sqrt{g_1^2+g_2^2}}|a>|n_1>|n_2-1>\exp(ik_1z_1) \quad - \quad \frac{g_1}{\sqrt{g_1^2+g_2^2}}|b>|n_1-1>|n_2>\exp(ik_2z_2)\right)$$

where |a> and |b> are the bare atom states, and $|n_1>|n_2>$ is a field state with n_1 photons at frequency ω_1 and n_2 photons at frequency ω_2. Here, g_1 and g_2 are the Rabi frequencies of the a<-->e and b<-->e transitions, proportional to $\sqrt{n_1}$ and $\sqrt{n_2}$, respectively. In the experiment to be described, the semiclassical limit applies, and the sum over photon number states can be replaced by a single state having the average photon number. Finally, k_1z_1 and k_2z_2 are the spatially dependent phases of the optical fields.

For equal Rabi frequencies, the trapped state reduces to:

$$(|a>|n_1>|n_2>\exp(i(k_1z_1-k_2z_2)) \quad - \quad |b>|n_1-1>|n_2+1>) \quad /\sqrt{2},$$

where the phase $\exp(ik_2z_2)$ has been factored out. In comparison, the high and low energy dressed states of the a<-->b microwave transitions are

$$(|a>|n_3>\exp(-ik_3z_3) \; - \; |b>|n_3-1>) \; /\sqrt{2}$$

and

$$(|a>|n_3>\exp(-ik_3z_3) \; + \; |b>|n_3-1> \; /\sqrt{2},$$

respectively, where ω_3 is the microwave frequency, and the semi-classical limit is again assumed.

To help clarify the physics involved, consider a stepwise process wherein the optical Raman interaction and the microwave interaction are separated in time. First, the optical Raman interaction puts the atoms into the trapped state, as illustrated in Fig. II-1(b). Next, the laser fields are turned off and a microwave field is turned on. In general, two microwave dressed states are possible, as shown by the energy level diagram of Fig. II-1(c). To determine into which microwave eigenstate the Raman trapped state evolves, it is necessary to know the relative phase of the microwave and the double optical (Raman) fields. This relative phase is given by

$$\phi = [(k_1z_1 - k_2z_2) - k_3z_3].$$

where it is assumed that all three states are in phase at $z_1 = z_2 = z_3 = 0$.

When the laser difference frequency is exactly in (or out of) phase with the microwave frequency, i.e., $\phi = 0$ (or $\phi = \pi$), the Raman trapped state translates directly into the high (or low) energy microwave dressed state. For any other value of the relative phase ϕ, a linear combination of microwave dressed states results. In such a case, Rabi spin flips occur[6] (largest for $\phi = \pi/2$), partially destroying the original dressed state. To detect the degree of microwave interaction, the microwave field can be turned off and the Raman interaction can be turned back on. Population lost from the trapped state would then appear as an increase in optical absorption.

Experimentally, this three step process can be realized using a separated field excitation scheme in an atomic beam. The experimental setup we used is illustrated schematically in Fig. II-2. Here, a sodium oven is operated at about 400°C to generate a thermal atomic beam. The laser field at frequency ω_1 (590 nm) is the output of a cw dye laser having 1 MHz of frequency jitter. To minimize the effect of this jitter[7], the field at frequency ω_2 is generated from that at ω_1 by using an acousto-optic modulator (A/O). The A/O is driven by a quartz stabilized microwave oscillator at the a<->b transition frequency

(1772 MHz). The laser fields at ω_1 and ω_2 are made copropagating to a high degree of precision by coupling both through a common single mode optical fiber (not shown). In this experiment, states |a> and |b> are the F=1 and F=2 hyperfine sublevels, respectively, of the $^2S_{1/2}$ ground state, and state |e> is the F=2 sublevel of the $^2P_{1/2}$ state. The laser beams in zones A and B are right circularly polarized, and a dc magnetic holding field of 0.3 Gauss is applied parallel to the laser propagation direction, to lift the degeneracy of the Zeeman sublevels. The $m=0$, $\Delta m=0$ Raman transition is used. For the microwave excitation, A TE_{201} rectangular resonant cavity is used in an orientation which excites the $m=0$, $\Delta m=0$ transition.

First, Raman excitation in zone A first pumps the atoms into the trapped state. Then, these atoms interact with a microwave field, zone M. The Raman probing interaction in zone B measures the degree of the microwave interaction by detecting any loss of the trapped state population, via the fluorescence detecting photodiode (PD). The pathlengths to zones A and B are set so that the optical difference frequencies in zones A and B are in phase[7]. The microwave field is generated by detecting and amplifying the beat between the two optical fields using a 2 GHz avalanche photo diode (APD). This ensures that the microwave and the double optical fields are phase locked. The relative phase ϕ

between the microwave and the laser difference frequencies is controlled by changing the pathlength traversed by the laser beams before reaching the APD.

Fig. II-3(a) shows the Raman-Ramsey fringes observed in zone B when the laser difference frequency is scanned, for zero microwave power. Fig. II-3(b) shows the fluorescence observed, with the laser difference frequency held exactly on resonance (fluorescence minimum), but the microwave power scanned. Here, the microwave field is exactly in phase with the optical difference frequency, i.e., $\phi = 0$. As can be seen, the microwave field has no effect, since in this case the optical Raman trapped state translates into a pure microwave spin-locked eigenstate. Fig. II-3(c) shows the case of $\phi = \pi/2$, as the microwave power is again scanned, with the laser difference frequency held on resonance. Here, the fluorescence depends strongly on microwave power, undergoing large oscillations caused by Rabi spin flips, indicating that a microwave eigenstate is no longer excited. The damping with increasing microwave power in Fig. II-3(c) is caused by velocity averaging effects. Comparison with the theoretical plots of Figs. II-3(d,e,f) shows good agreement[8]. To illustrate what happens for phases other than $\phi = 0$ or $\pi/2$, Fig. II-4(a) shows the absorption observed when the phase ϕ is rapidly varied while scanning the microwave power. Here, the

absorption varies sinusoidally with ϕ, and the curves of Fig. II-3(b) and II-3(c) form the envelope function. Fig. II-4(b) shows the corresponding theoretical plot.

We also performed the complimentary experiment wherein a microwave field is used to excite the optical Raman trapped state. This involves replacing the first Raman zone in Fig. II-2 by an optical pumping zone (not shown), which effectively puts all the atoms into state $|b\rangle$ before entering the microwave cavity. For a microwave power corresponding to a $\pi/2$ pulse, the resulting state is

$$(-i \quad |a\rangle|n_3\rangle \exp(-ik_3 z) \quad + \quad |b\rangle|n_3 - 1\rangle) \quad /\sqrt{2}.$$

This can be made to correspond to a Raman trapped state if the relative phase ϕ between the microwave and the laser difference frequency is $\pi/2$.

Experimental evidence of microwave excitation of an optical Raman trapped state appears in Fig. II-5. Here, Fig. II-5(a) shows the zone B fluorescence[9] obtained by scanning the laser difference frequency with a microwave power corresponding to a $\pi/2$ pulse and a relative phase of $\phi = \pi/2$. As can be seen, Ramsey fringes are obtained which closely resemble those in Fig. II-3(a), even though only one Raman excitation zone is present. Thus, an optical Raman trapped state has been excited by

the microwave field. For completeness, Fig. II-5(b) shows the zone B fluorescence obtained with the microwaves turned off. As expected, no Ramsey fringes are seen in this case.

Extension of these results to a single zone excitation scheme (where both microwave and optical Raman fields are present simultaneously) is also of interest because of the possibility of exciting a three photon trapped state[10]. This would occur for a relative Raman and microwave phases of $\phi = 0$ or π. For other values of ϕ, all dressed states are partially optically absorbing, where the steady state absorption depends on ϕ. For a properly chosen configuration, the position dependence of the relative phase ϕ would result in a grating being produced, which would diffract both optical and microwave fields. Numerous applications of this effect can be imagined if the microwave transition is replaced by a mm-wave or far infrared transition. For example, real time mm-wave beam steering can be performed wherein the mm-wave could be deflected by the optical beams. It should also be possible to perform real time holographic far infrared to visible image conversion[11].

Finally, we briefly consider the effects of the finite photon number spread. Because of this spread, dressed states exist in manifolds, each characterized by the photon number. In case of a microwave excitation, the manifolds are not coupled due to

lack of spontaneous emission. Addition of the Raman field partially restores the manifold. For example, a relative phase of $\phi = \pi$ would cause the weak field seeking microwave state to decay to decay into the strong field seeking state at a rate which depends on the laser intensity. This process may have applications to collision studies, laser cooling, and possibly even to trapping of neutral atoms in a microwave cavity[12]. We are currently investigating some of these applications potentials.

In summary, we have used a laser induced resonance Raman transition—in a sodium beam to excite individual dressed states of the microwave-spin hyperfine transition. Conversely, we have also used the microwave interaction to excite the Raman trapped state. Extension of this technique to mm-waves or to the far infrared may lead to applications such as beam steering and image conversion.

References -- part II

[1] H. R. Gray, R. M. Whitley, and C. R. Stroud, Jr., Opt. Lett. 3, 218 (1978).

[2] S. R. Hartmann, E. L. Hahn, Phys. Rev. 128, 2042 (1962).

[3] Y. S. Bai, A. G. Yodh, and T. W. Mossberg, Phys. Rev. Lett. 55, 1277 (1985).

[4] G. Alzetta, A. Gozzini, L. Moi, and G. Orriols, Nuovo Cimento **36B**, 5 (1976).

[5] P. M. Radmore and P. L. Knight, J. Phys. B. **15**, 3405 (1982)

[6] N. F. Ramsey, **Molecular Beams**, (Oxford U. Press, London, 1956).

[7] J. E. Thomas, P. R. Hemmer, S. Ezekiel, C. C. Leiby, Jr., R. H. Picard, and C. R. Willis, Phys. Rev. Lett. **48**, 867 (1981).

[8] The microwave field amplitude scan was non-linear, as indicated in the horizontal axes of Figs. 3(b,c,e,f).

[9] Lock-in detection was employed to enhance signal to noise for this data.-

[10] S. J. Buckle, S. M. Barnett, P. L. Knight, M. A. Lauder, and D. T. Pegg, Optica Acta 33, 1129 (1986)

[11] For other techniques of laser assisted far infrared to visible image conversion, see for example: V. V. Krasnikov, M. S. Pshenichnikov, and V. S. Solomatin, Sov. J. Quan. Elec. **14**, 418 (1984), and the references therein.

[12] C. Agosta, I. Silvera, H. Stoof and B. Verhaar, Phys. Rev. Lett. 62, 2361 (1989)

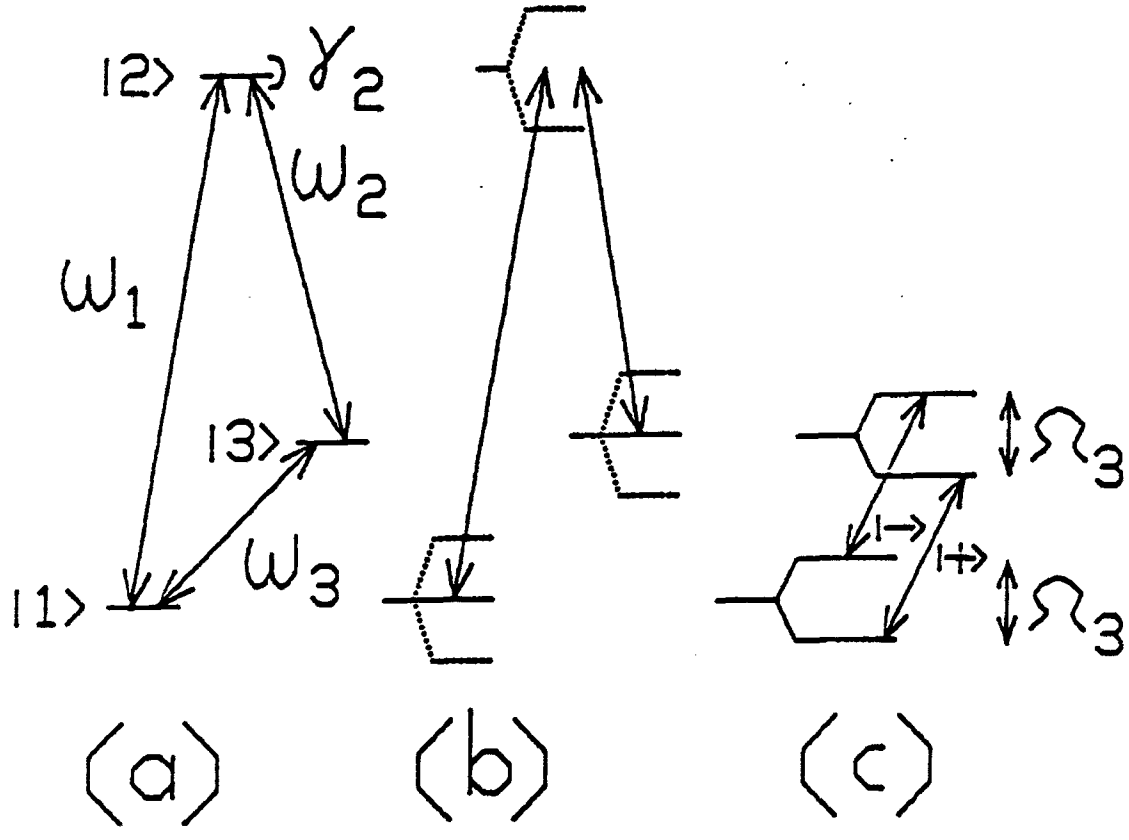

Fig. II-1 (a) A three level atomic system in the Λ configuration. (b) Dressed states for the resonance Raman interaction. The trapped state is denoted by the solid lines. (c) The microwave spin-locked (dressed) states.

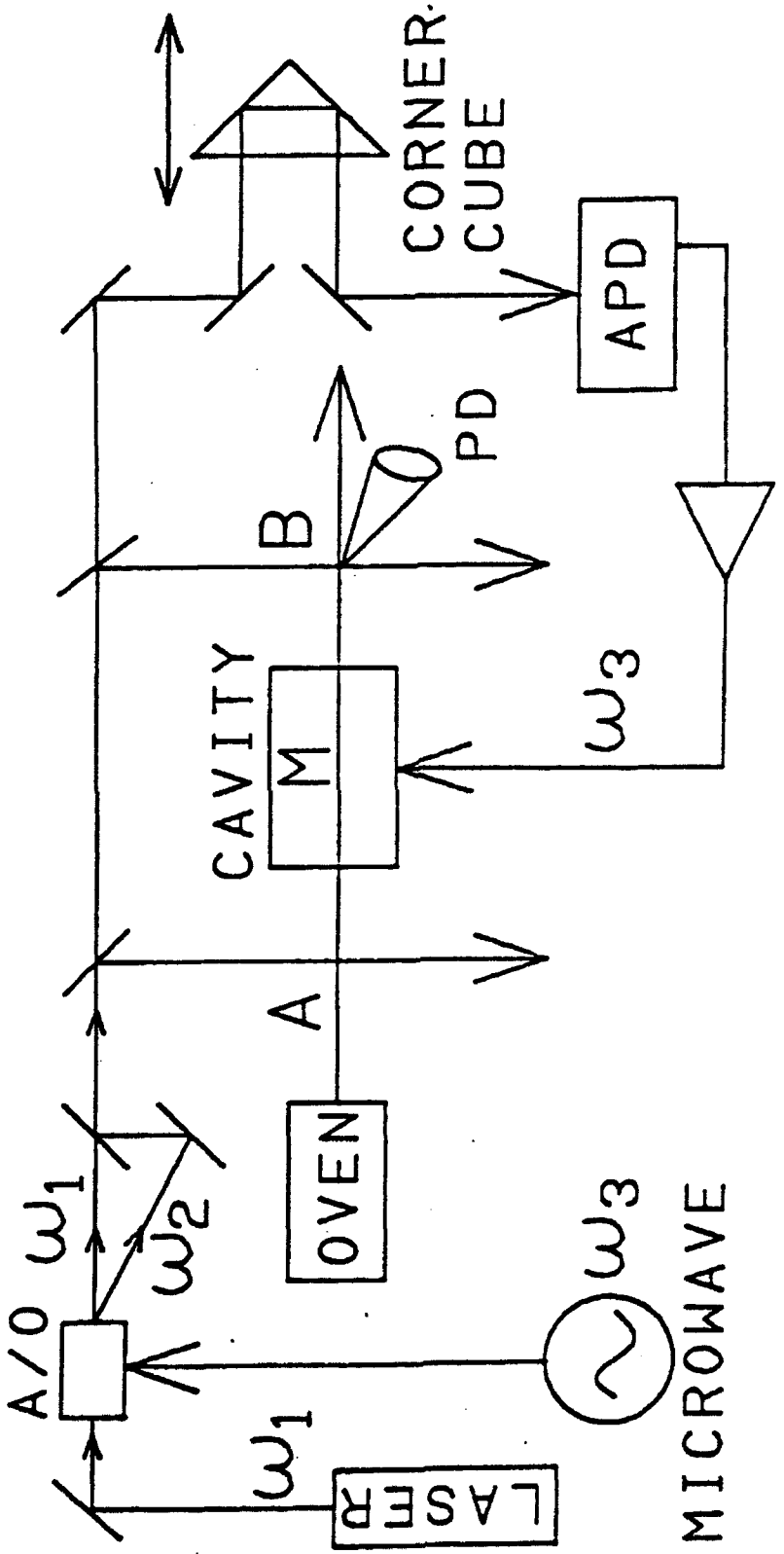

Fig. II-2 Schematic diagram of the experimental setup.

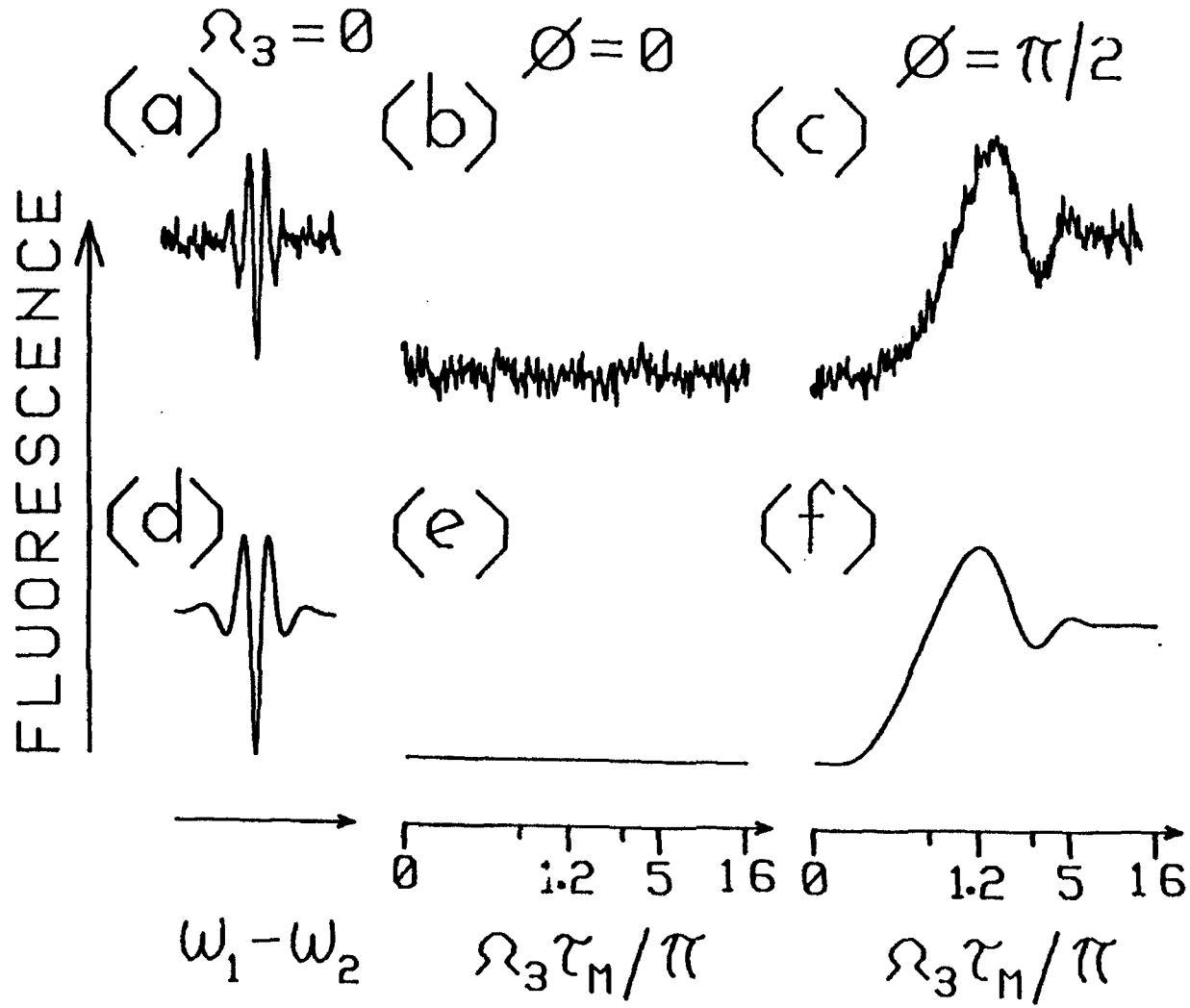

Fig. II-3 (a) Ramsey fringe pattern in absence of microwave. (b) Zone B fluorescence as a function of microwave power (in units of π pulses), for a relative phase of $\phi = 0$. (c) for $\phi = \pi/2$. (d, e & f) Theoretical plots for (a, b & c) respectively.

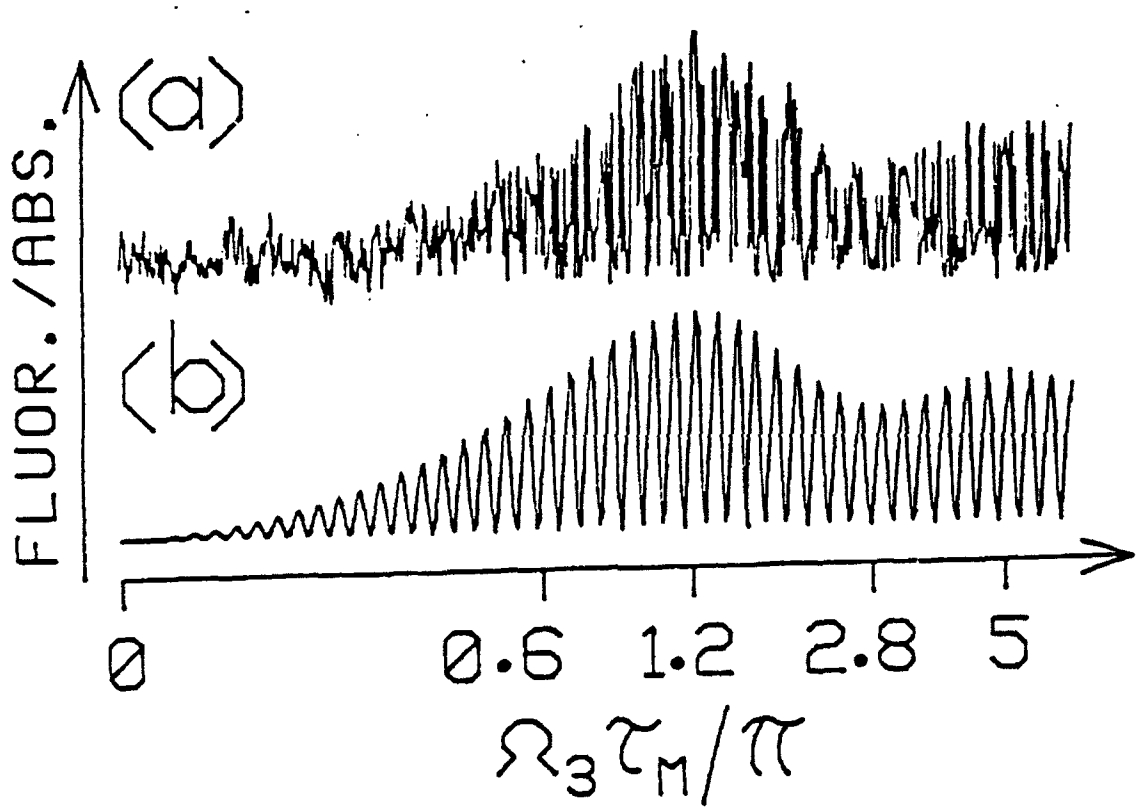

Fig. II-4 (a) Zone B fluorescence as a function of microwave power, while the relative phase ϕ is rapidly scanned. (b) Corresponding theoretical plot.

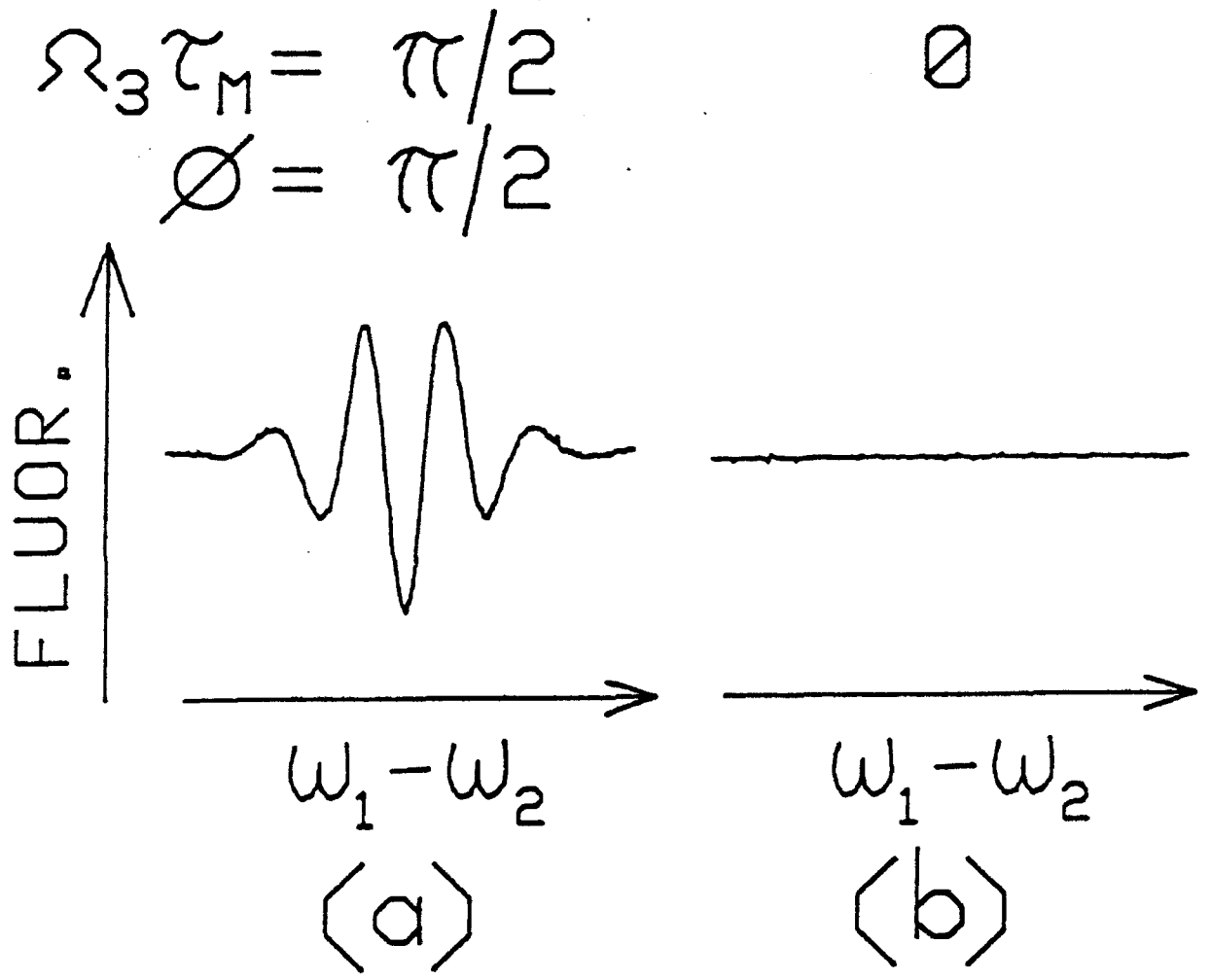

Fig. II-5 (a) Microwave-Raman interference (Ramsey) fringes, generated for a relative phase of $\phi = \pi/2$ and a microwave $\pi/2$ pulse (b) The fringe disappears for zero microwave power.

(III) Optically Excited Microwave Spin Echoes

There has been much recent interest in the use of optical photon echoes for information storage and processing[1]. However, experimental demonstrations have so far been restricted to spectral hole burning materials operating at liquid He temperatures. Information has been stored using microwave spin echoes in room temperature materials[2], but the data rates and storage densities achievable are orders of magnitude below those of optical echo techniques. The proposed scheme, which makes use of an optically excited microwave spin echo, is capable of data rates and storage densities comparable to the optical echo techniques, but potentially at much higher temperatures (provided a suitable material can be found). In contrast to multilevel optical echoes, the Raman excited microwave coherences can store information which is spread over times much longer than the homogeneous decay time of the optical coherence.

The basic architecture of the proposed scheme is illustrated in Fig. III-1. A three level system is used, which can be excited by two near resonant optical transitions (resonance Raman) or one near resonant microwave transition. As shown, information is first input as an optical pulse train (two unequal amplitude pulses in the figure). The optical input beam contains both optical frequencies needed to excite the resonance Raman

transition. The Raman interaction creates a coherence which depends on phase differences in the two optical frequencies. This phase sensitivity, combined with dephasing of the ground state coherence due to inhomogeneous broadening, allows both the temporal and phase information contained in the optical fields to be stored via a process analogous to spectral hole burning. To recall this information, a π-pulse must be applied. Since the Raman coherence directly translates into a microwave coherence[3] this can be accomplished with a microwave π-pulse. The ground state coherences will then rephase at the appropriate time where they can be detected optically, as bright and dark areas, using an optical Raman probe, as shown in Fig. III-1.

The experimental demonstration is accomplished using a sodium atomic beam with three interaction zones. In the first zone, two spatially separated optical Raman pulses are used, as illustrated in Fig. III-2(a). This represents a temporal pulse sequence because the atoms are moving. A uniform magnetic field is applied in this zone, which produces an inhomogeneous broadening because of the axial velocity distribution in the thermal atomic beam. In the second zone, a microwave π-pulse is used to time reverse the spin coherence. The third zone consists of a Raman probe pulse (Fig. III-2(b)) to detect the coherence optically. In order to generate the echo, a magnetic field is applied in this zone, which is matched to that in the first zone.

The observed echo signal is shown in Fig. III-2(c). As shown, the time separation between the pulses is many times larger than the lifetime of excited sodium (16 nsec. for the D_1 transition).

References -- part III

[1] M.K. Kim and R. Kachru, **Opt. Lett.** 12, 593 (1987)

[2] S. Fernbach and W.G. Proctor, **Jour. of Appl. Phys.** 26, 170 (1955)

[3] M.S. Shahriar and P.R. Hemmer, **Phys. Rev. Lett.** 65, 1865 (1990)

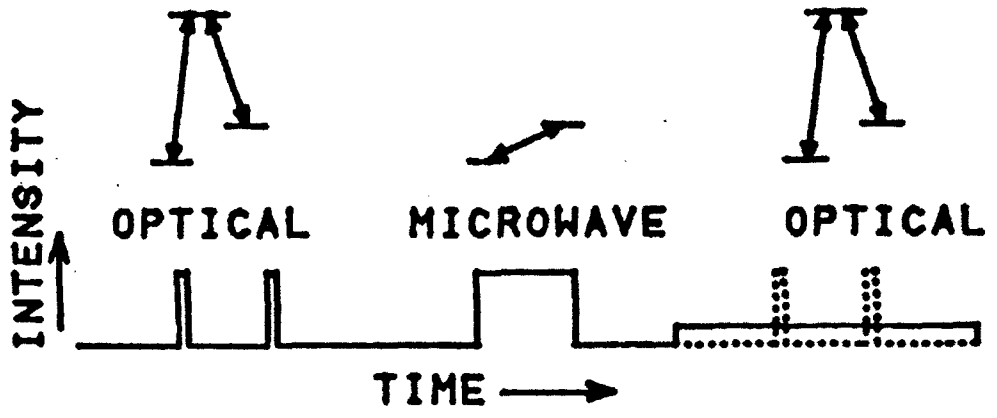

Fig. III-1 Schematic showing proposed architecture for optical data storage with Raman-microwave spin echoes. The dotted lines on the right side show the microwave spin echoes which are detected by an optical Raman probe (superimposed solid line).

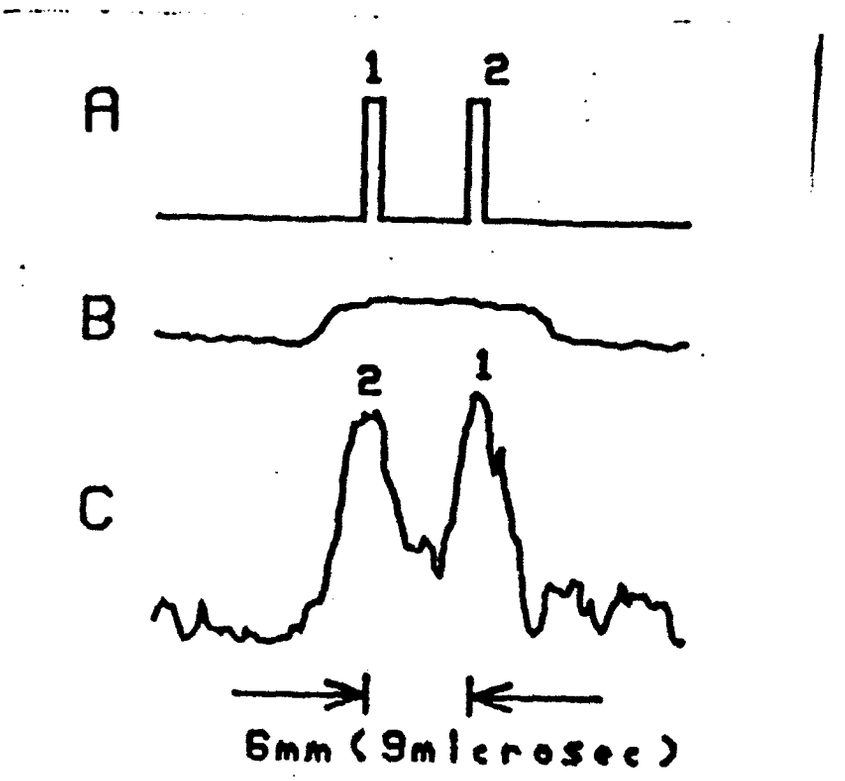

Fig. III-2 (a) Input optical pulse train. (b) Raman probe envelope. (c) Optically detected microwave echo pulses. Note time reversal in echo.

Thesis

Selim M. Shahriar, "Fundamental Studies in Three Level Atoms and Applications," **Ph.D in Electrical Engineering and Computer Science**, October 1991.

Publications

1. S. Shahriar, P.R. Hemmer, "Microwave-Phase-Dependent Optical Absorption," in **International Quantum Electronics Conference 1990 Technical Digest Series** (Opt. Soc. of Am., Washington DC) QFA6.

2. S. Shahriar, P.R. Hemmer, "Direct Excitation of Microwave-Spin Dressed States Using a Laser-Excited Resonance Raman Interaction," **Physical Review Letters 15**, 1865 (1990)

3. S. Shahriar, P. Hemmer, N. Bigelow and M. Prentiss, "Forces on Three Level Atoms Including Trapped State Contribution," in **Quantum Electronics and Laser Science 1991 Technical Digest Series** (Opt. Soc. of Am., Washington DC) pp 186.

4. M. G. Prentiss, N. Bigelow, M. S. Shahriar, P. R. Hemmer, K. Berggren, J. Mervis, S. Ezekiel, **Enrico Fermi International School of Physics Course CXVIII**, "Laser manipulation of Atoms and Ions," Milan, Italy (July 1991).

5. M. Prentiss, N. Bigelow, S. Shahriar and N. Bigelow, "Forces on Three Level Atoms Including Coherent Population Trapping," **Optics Letters**, 16, 1695 (1991).

6. P. Hemmer, M. Prentiss, S. Shahriar and P. Hemmer, "Optical Force on the Raman Dark State in Two Standing Waves," accepted for publication in **Optics Communications**.

7. P. Hemmer, S. Shahriar, M. Prentiss, D. Katz, K. Berggren, and J. Mervis, "Observation of the Deflection of Three Level Atoms due to Two Standing Wave Optical Fields," **Quantum Electronics and Laser Science Conference**, 1992, accepted.

8. P. Hemmer, S. Shahriar, M. Prentiss, D. Katz, K. Berggren, and J. Mervis, "First Observation of Forces on Three Level Atoms in Raman Resonant Standing Wave Optical Fields" accepted for publication in **Physical Review Letters**.

9. M. Prentiss, D. P. Katz, J. Mervis, K. Berggren, P. Hemmer, S. Shahriar, N. Bigelow, "Damping and Deflection of Three Level Atoms due to Two Standing Wave Optical Fields, and Application to Traps," **International Laser Science Conference**, 1992, invited paper

10. S. Shahriar and P. Hemmer, "Optical Data Storage with Raman Excited Microwave Spin Echoes," submitted to OSA Conference, 1992

*U.S. GOVERNMENT PRINTING OFFICE: 1993-710-093-60171